27/06/2016

Theoretical tool box for a better catalytic understanding

Authors : Michel Waroquier, Kristof De Wispelaere, Julianna Hajek, Sven Rogge, Jeroen Van Der Mynsbrugge, Veronique Van Speybroeck

Center for Molecular Modeling , Ghent University, Technologiepark 903, B-9052 Zwijnaarde, Belgium

1. Introduction

Theoretical modeling has nowadays taken an indispensable role in many fields of science and engineering, thanks to the availability of systematically stronger computing power and the steady development of new ingenious theoretical methods and numerical implementations. Within the field of catalysis, modeling has also taken a prominent role. A lot of experimental papers are combined with computational modeling to explore issues such as the nature of the active site, the determination of reaction rates at the single reaction level,…. These are typically questions which are very hard to assess purely from experimental point of view. Theory can thus be used to explain and rationalize experimentally observed features. However the field has evolved substantially and theory has now come to the point where it can even be used in a predictive manner. Nice examples are high-throughput screening studies, where a large database of hypothetical materials is screened for desirable properties. Seminal studies of this kind were published by the group of Snurr, Smit,….[1-4] Such efforts may lead to the design of dedicated experiments on a set of promising materials. Ideally theory could answer important questions related to activity, selectivity, and stability of the catalyst. However one must be realistic, despite the enormous progress made during the last decades, computational catalyst design still needs to overcome many hurdles in order to be used as an all-in toolbox. Many issues are related to the typical length and time scales encountered in a catalytic process. The overall function of a catalyst is the interplay between many multi-scale phenomena both in space and time. This was nicely illustrated by Weckhuysen in his review on spatial heterogeneities in catalytic solids.[5] In this book chapter we give our view on the question whether we dispose anno 2016 of a theoretical tool box for a better catalytic understanding.

To answer these questions, one must also define its expectations. Until recently the catalytic community was satisfied if theory succeeded in suggesting some plausible reaction schemes and could reproduce qualitatively experimental findings. However with the rapid evolution of the field, the expectations have currently taken a whole other dimension. Nowadays, methods are developed and explored to reach chemical and kinetic accuracy for reaction enthalpies and rate constants.[6-8] In some cases this has proven to be achievable, but at the expense of a serious computational cost, which hampers its applicability as mainstream methodologies. Furthermore such reliable predictions from theory also request the availability of very accurate experimental data. For example to predict reaction rates with kinetic accuracy – i.e. within a factor 10 from the experiment – one needs to dispose of experimental data that provide the chemical kinetics for a single reaction within an often very complex reaction network. Thus the development of such accurate methods imposes also challenges for the experimentalists to generate data which are comparable with the produced theoretical data.

Next the catalyst should be studied at work, thus at operating conditions.[9] This imposes a huge challenge for theory as this requires models that account for realistic process conditions involving actual reaction temperatures, pressures, loading of the guest species, and other degrees of freedom. One can imagine that in these circumstances the catalytic process becomes very complex and one cannot resort anymore to the textbook concept of a single transition state and a restricted number of configurations on the potential energy surface. Very recently new methods are being explored within the field of computational catalysis, such as enhanced molecular dynamics methods which allow sampling the free energy surface at operating conditions.[10-23] However this field is in full exploration and new methodologies are being developed to apply advanced molecular dynamics techniques in the field of catalysis.

In this book chapter we will focus on heterogeneous catalysis and in particular catalytic reactions taking place in the pores of a nanoporous material. Due to the heterogeneous character of the chemical process the complexity of the reaction also increases. Such applications are a good value indicator to assess the available toolbox of techniques and algorithms. We will concentrate on catalytic reactions taking place in two types of nanoporous materials: zeolites and metal-organic frameworks (MOFs). Zeolites are crystalline framework structured alumino-silicates with pores and cages of molecular dimensions (< 2 nm). Their characteristic pore dimensions , high surface area, porosity, diversity… make them very tractable in a wide scope of applications [24] making zeolites the workhorses of today's chemical industry. MOFs are hybrid nanoporous materials build from inorganic moieties connected with organic linkers (Figure 1). These last materials have a more recent history and their probable catalytic potential is still under exploration. This class of new materials knows a still increasing interest from the community due to its building block concept resulting to a tunable composition and structural diversity combined with a high porosity. These properties lead to a broad variety of applications varying from adsorption and gas storage, separation, optics and sensing to catalysis. [25-27] Catalysis will probably not evolve to the most promising property of MOFs, the other properties also need an appropriate description of the metal sites with emphasis on its accessibility.

The computational toolbox which is available nowadays – with its strengths and limitations – can certainly not be used as a black box. Even though a lot of programs are currently available for a large community, computational catalysis requires the knowledge of an advanced user, who masters the strengths and the weaknesses of current computational methods. The whole modeling procedure consists of various steps which each merits special attention to reach the final objective of an optimal tool to describe heterogeneous catalysis in all its complexity.

A good modeling trajectory should fulfill many criteria and should cover many features. First, it is essential to model the catalyst's active site by fully taking into account the effects of the molecular environment. Next, the adsorption of the reactants at the active site and the reaction itself should be studied. The latter encompasses the determination of the transition state(s), calculation of the reaction rate constant and identification of the various factors governing the reaction rate.

In this contribution focus lies on the adequacy of contemporary state-of-the-art techniques present in the current tool box to achieve the highest reliability, reproducibility and accuracy in the description of catalytic reactions in the pores of a nanoporous material. We realize that this is a

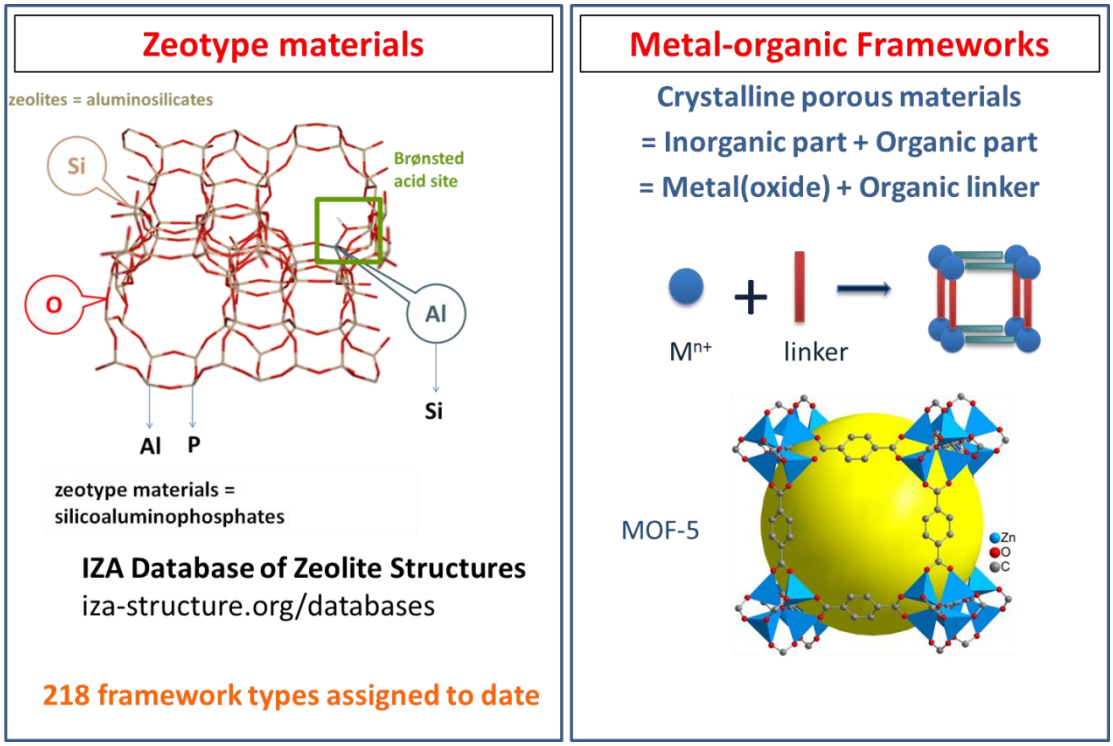

Figure 1: Schematic of the versatility of nanoporous materials. By combining different building blocks a wide variety of zeotype materials and metal-organic frameworks can be synthesized.

rapidly varying and steadily progressing issue, but for any reader such an overview remains an instructive exercise, reporting the good performing features, the issues that are subject to improvement and some critical notes of present modeling tools. Some similar exercise has been presented by Joachim Sauer and Hans-Joachim Freund [9] discussing the hierarchy of model studies on catalytic reactions with increasing complexity.

We will focus on some particular items that took our attention starting from our own expertise in modeling heterogeneous catalysis. It encompasses the models to describe the catalytic site including all ingredients which could have a significant effect on the reaction. This contribution also tries to discuss carefully the advantages/disadvantages of static approaches versus dynamic models. Modeling of a reaction always starts from a reactive complex, but the construction of such a complex requires a lot of attention as it determines for a large part the initial stages of the reaction path on the free energy surface. A special section is devoted on the determination of chemical kinetics of the catalytic reaction and thus identification of the transition state (TS) or transition state region which constitutes one of the major objectives of a modeling tool box. Finally, computational spectroscopy has reached such a level of accuracy that it assists in interpreting in-situ spectroscopic measurements which are indispensable for characterization of reaction intermediates.

2. Modeling the catalytic active site

2.1 Taking into account topology

An important issue when modeling catalytic processes in nanoporous materials is to select an appropriate model to simulate the extended molecular environment of the material itself. We first illustrate this point for zeolites. Zeolites are bulky materials with a large amount of atoms and thus computationally accurate methods need to be used to account for a representative fraction of the material within a reasonable computational time. The first attempts over the years to model the active site in a **zeolite** framework are based on small clusters containing a limited number of tetrahedral atoms (illustrated by a 1T and 5T cluster in **Figure 2a,b**). The main advantage of such small clusters is their limited number of atoms, which allowed usage of very accurate electronic structure methods for the calculation of the energy of the system. Although they have shown their practical use in times where computational resources were rather limited by giving some valuable qualitative insight, they are no longer of any use in current models as the topology is completely neglected. In a next generation more extended clusters are considered. A finite cluster is cut from the periodic structure of the material which needs to be sufficiently large to account properly for the topology. **Figure 2c** shows 3D-views of a finite cluster model (46T) corresponding to the MFI topology. Typically, such clusters are terminated by hydrogen atoms which are fixed in space to prevent the unphysical collapse of the cluster during geometry optimization. This of course leads to the drawback that the flexibility of the nanoporous material is not fully exploited. Another shortcoming is that extended clusters containing many atoms become computationally hardly manageable with very accurate quantum chemical methods. To prevent this computational bottleneck, multilayer approaches such as ONIOM and other QM/MM methods were introduced. [8, 21, 28-33] The ONIOM method was used in the work of Maihom et al. [28] to model reactions in H-ZSM-5. These authors considered an 128T cluster, in which only 12 T atoms were treated at the DFT level for reasons of computational efficiency. The rest of the cluster was modeled using the universal force field (UFF) and during the geometry optimization only a small portion of the cluster was relaxed. To mimic the electrostatic effect of the remainder of the infinite zeolite lattice, the clusters were further embedded in a set of point charges to reproduce the zeolite Madelung potential.
In addition the accuracy of all these QM/MM schemes largely depends on the cluster size, QM method – for Density Functional Theory (DFT) more specifically the exchange-correlation functional – and the basis set, as pointed out by Bell and co-workers [31]. Therefore, use of cluster models requires a thorough benchmark for each system and for each property of interest. In any case cluster models give a rather limited view of the material, since flexibility is not accounted for.

A still valid and interesting advantage of cluster models is that numerical algorithms to search for transition states are better developed than in solid state codes which are typically used for periodic representations of the crystal lattice. A procedure which is often used to remedy this issue is to localise a transition state in a cluster model and transfer it afterwards to a periodic model. As such good initial guesses for transition states in periodic models are obtained, which may help to localise the transition state in the periodic model.

Alternatively, the nanoporous material can be best represented by a periodic model. In such periodic representation of a nanoporous material, one or more unit cells of the framework are included in

the model. **Figure 2d** displays a periodic model of the well-known MFI material. Use of periodic models to mimic the periodic structure of the material is by definition the most appropriate way to simulate the active site, as all ingredients characterizing the active site such as its location in the pores of the nanoporous material, the shape of the pores and channels, flexibility of the frame, etc. are taken into account in a natural way. Periodic calculations of framework materials are typically conducted with codes that find their origin in solid-state applications.

Both in cluster and periodic based models, Density Functional theory (DFT) is the method of choice to treat the systems of interest thanks to their favorable balance between accuracy and computational efficiency. For periodic based calculations one still uses in many cases the so called gradient corrected functionals as they have proven their merits for true solid state systems. Use of hybrid functionals or more advanced functionals (metahybrid functionals,...) is currently implemented in most of the periodic codes (VASP, CRYSTAL, ...) but still very demanding in geometry optimizations of the periodic cell and thus not systematically applied.

As long-range electron-electron interactions are not involved in commonly applied local density functionals they have to be inserted separately. In most of the cases Grimme D3 dispersion corrections were used.[34]

It is not the intention to give a full overview of all electronic structure methods currently available, as this would entail a review on its own. However we refer to some dedicated reviews and other interesting references on the topic. [23, 35]

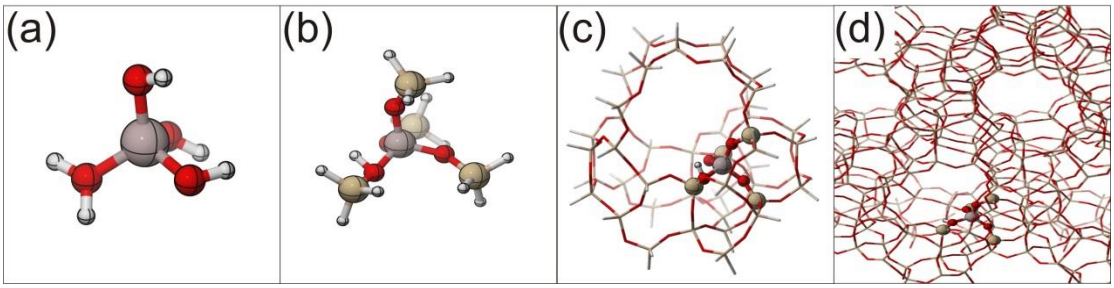

Figure 2: Illustration of various models to account for the zeolite topology: a 1T cluster (a), a 5T cluster (b), a 46T cluster for H-ZSM-5 (c) and the periodic structure of H-ZSM-5 (d) with indication of the acid site. Adapted from ref. [23] with permission from The Royal Society of Chemistry.

2.2 Determining the nature of the active site

One of the challenges in modelling catalysis in nanoporous materials consists in determining the nature of the active site. Catalysis in zeolites takes place in the surroundings of an active site such as a Brønsted acidic center originating from a charge compensating proton at an aluminium substitutional defect in the zeolite framework or at an extra-framework Lewis acid site. Metal-exchanged zeolites received considerable attention in catalysis. Some examples are the Cu-SSZ-13 material which has been studied for processes such as the ammonia-assisted Selective Catalytic Reduction (NH_3-SCR) of NO_x or Ti substituted zeolites which proved to be effective and versatile partial oxidation catalysts. [36] These are only a limited number of examples from the wealth of

literature available on the topic. For more detailed discussions we refer to one of our recent reviews. [35] There we pointed out that for these metal exchanged zeolites, it is very complex to elucidate the true nature of the active site and we demonstrated the added value of modelling to resolve these issues. Within this book chapter we will focus on examples taken from Brønsted acidic zeolite catalysis. **Figure 3** shows a schematic representation of a zeolite model in which a Brønsted acidic site is incorporated and a Lewis acidic site is present.

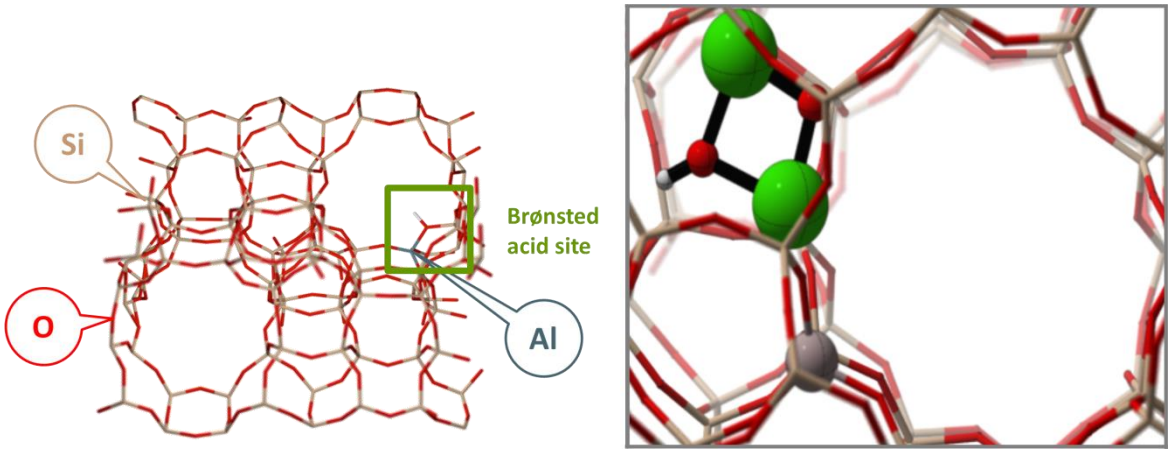

Figure 3: Brønsted acid site (BAS) in H-ZSM-5 with an Al substitution and the charge compensating proton (left) ; Lewis acidic site by the presence of charge compensating Ca cation. After modification with Ca, ZSM-5 can contain $CaOCaOH^+$ species at the Al substitution. Figure adapted from ref. [37] with permission from Wiley.

Modelling of the active site is not that trivial as could be expected at first sight. There are also some challenging issues that have to be taken into account. In most modelling studies on Brønsted acidic zeolites, one acid site is taken into consideration in the molecular model. A first question concerns however the position of this acid site. Aluminium siting in zeolite materials is a fairly complex problem in itself; for example, for H-ZSM-5, the distribution of aluminium has been shown to depend mainly on the method and conditions that are applied for the synthesis of the catalyst.[38-40] As a result, the selection of a single active site remains somewhat ambiguous. In many cases more pragmatic choices are made. A reasonable selection consists in retaining only those aluminium substitutions that give rise to acid sites which are accessible to the reactant and thus for which enough space is available to host the various transition states. In case of the H-ZSM-5 material, one often positions the acidic site at the T12 position, located at the intersection of the straight and sinusoidal channels as this position ensures enough place for the reactions to take place. Furthermore once the aluminium is placed in the framework, one could select the bridging hydroxyl groups with highest acid strength or with lowest deprotonation energy. This approach has frequently been used in literature. [7, 41, 42]

Another factor that complicates the accurate description of the active site is the presence of high loadings of protic molecules in the surroundings of a Brønsted acid site. It has been found that sufficient amounts of water or methanol molecules are able to deprotonate a zeolite's Brønsted acid site at operating conditions with the formation of protonated water or methanol clusters as depicted in **Figure 4**.[11-14, 43-51] These protonated clusters might in their turn initiate reaction;

however such clusters exhibit a distinct intrinsic reactivity (vide infra). Such effects can be studied with advanced molecular dynamics techniques as described further in this chapter.

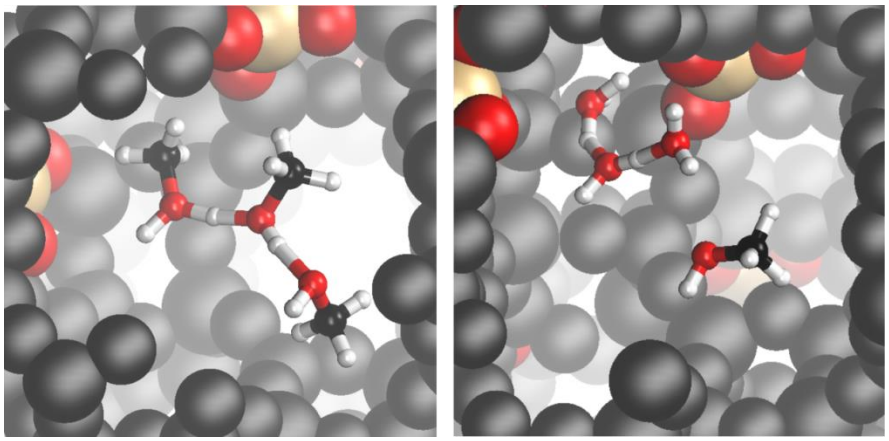

Figure 4: Protonated methanol (left) and water (right) cluster occupying a Brønsted acid site of H-SAPO-34 at 330 °C and around ambient pressure.

Determining the nature of **the active site within MOFs** has proven a true challenge as in many materials catalytic active sites are created by intentional creation of defects. These defects do increase the accessibility of the active sites, which in most cases represent Lewis acid centers formed by the metals of the MOF. From a molecular modeling point of view, we must also need to explore the advantage and the usefulness of the active site in the course of the reaction under study. We illustrate this concept for some Lewis catalyzed reactions in MOFs and more in particular for the UiO-66 type of material consisting of $Zr_6O_4(OH)_4$ inorganic building blocks and terephthalate linkers. This Zr(IV)- based MOF received considerable attention [52-54], as the UiO-66 material possesses a high thermal and chemical stability. Windows with a diameter of about 6 Å guarantee the accessibility to the cages. For Lewis catalyzed reactions it was demonstrated that terephthalate defects are responsible for the catalytic activity in UiO-66 [27, 55]. Moreover catalytic performance could in many cases be improved by functionalization of the linkers. It is a challenge for the theory whether the current techniques in the current tool box succeed in reproducing the catalytic activity as measured in diverse experiments.

Most of the experimental investigations on catalytic performance of MOFs are concentrated on oxidation reactions [27] and other reactions like the citronellal cyclization [56] where the catalytic activity is concentrated around the metal which acts as a Lewis acid site.

Defect sites can be created by linker deficiencies increasing the Lewis acid strength and making the metal center more accessible for potential reactant molecules. Determining the structure of the defect site or active site has proven a true challenge both for experimentalists as theoreticians, as the type of a deficiency in UiO-66 can be very broad varying from a missing linker to a missing Zr brick [57]. Removal of a benzenedicarboxylate (BDC) requires a charge balancing species. By means of single crystal X-ray diffraction (SXRD), the presence of two hydroxyl group terminations and/or coordinating water molecules has been observed.[58, 59] Trickett et al. postulated the presence of an extra hydroxide anion per defect site, bringing the total amount of defect coordinating water units on 3. Recently a variety of theoretical studies appeared which are based both on static and

molecular dynamics first principle calculations both on clusters and on periodic models to unravel the nature of the active site and the coordination of water to the defect sites. [60, 61]

Catalytic reactions on UiO-66 type of materials have been very successfully modeled using extended cluster models. We illustrate in **Figure 5** an extended cluster for UiO-66 and UiO-66-NH_2 where only four linkers are explicitly retained in the cluster to surround the active site. The remaining seven linkers were replaced by formic groups. Note that the extended cluster is constructed from a unit cell with one terephthalate defect, resulting to two active Zr-sites with coordination number 7. These Zr-sites operate as Lewis acid sites and are encircled with green circles. Analogously, UiO-66-NH_2 was constructed by replacing a hydrogen atom by an amino group on each phenyl ring. These amine groups act as Brønsted base sites and indicated with pink circles in **Figure 5b**. These cluster models have shown their usefulness [56] but in a sense they are also limited. The cases we studied so far showed that such extended models are in many cases sufficient to describe the different reaction steps mechanistically as all directly involved ingredients to go ahead with the reaction are present, but subtle factors generated by the environment represented by the linkers not involved in the cluster, framework flexibility or presence of assisting water molecules are not taken into account. If such factors are drastically affecting the mechanism or reaction rates, one can anticipate that such extended cluster models will not be able to reproduce these effects. We foresee that with the near future due to improvements of theoretical models and steady increase in computational power, more catalysis work within MOFs using periodic models and state of the art quantum mechanical models will be performed.

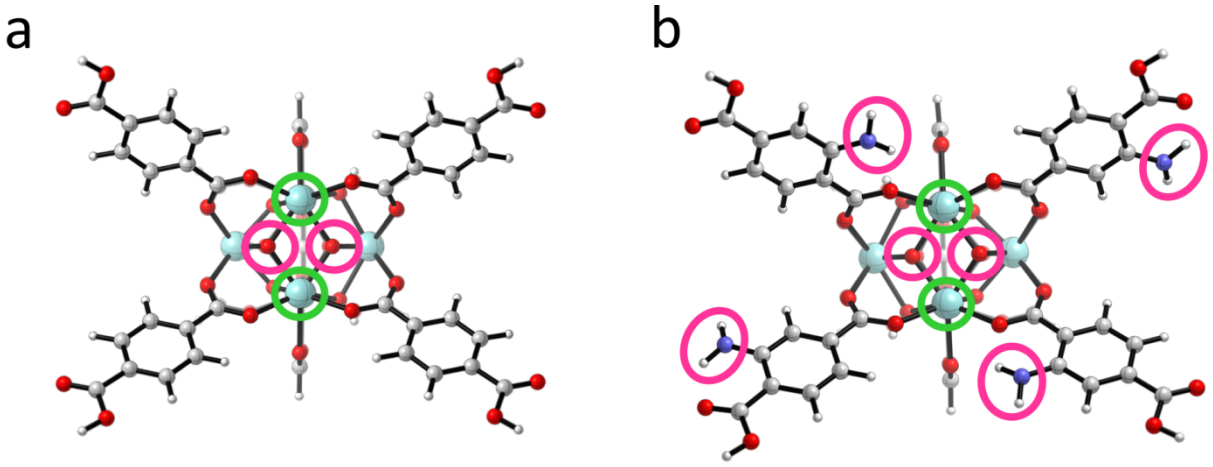

Figure 5: Cluster model with a Lewis acid site (encircled by green circles) and a Brønsted base site (encircled by pink circles) in UiO-66 and UiO-66-NH_2 with one linker defect. Taken with permission from ref. [56]

Indeed as in zeolites the most appropriate model to describe a MOF is the periodic model. Unit cells of the periodic MOF structures may be of respectable size and at the limit of actual feasibility. To illustrate, **Figure 6** shows the unit cell of a UiO-66 containing four inorganic Zr-bricks $<Zr_6O_4OH_4(RCOO)_{12}>$ and 24 BDC (terephthalate) linkers. $RCOO^-$ is a shorthand notation for half a BDC^{2-} linker. The coordination of each Zr-brick is twelve-fold. UiO-66 can only be catalytically active if linker defects are present. In **Figure 6** we visualize the unit cell of a two-linker defect generating Zr-

bricks with coordination number CN_1=12, CN_2=10, CN_3=12 and CN_4=10. The conventional unit cell with two linker defects counts 456 atoms – 2 x 18 atoms = 420 atoms among which 24 Zr-atoms. This already gives an indication of the required computational cost. A geometry optimization with the periodic code VASP [62-65] for such an extended system with addition of frequency calculations demands a huge computation time but is presently in principle feasible. To reduce the computational time a periodic unit cell consisting of only two Zr-bricks can be considered, which has been applied with success [56] but has of course its limitation as only a particular class of defect structures can be incorporated in this reduced periodic cell and periodic images are manifestly closer to each other which generate unphysical perturbations. This is best visualized in **Figure 6**. In literature most of the modeling activities on MOFs go to the description of their structural and thermal properties. Only a few papers deal with modeling of a chemical reaction with the MOF as catalyst. Catalytic reactions in MOFs are not so abundant in literature and not so widely used as in zeolite catalysis. Another reason of this lack on theoretical work lies probably on the limitations of the cluster model and the too large unit cell for an adequate modeling of the active site. However, we demonstrate that the active site of a MOF can nowadays best be modeled by its periodic 3D structure. Linker deficiencies lead to Zr-bricks with different coordination numbers. Current modeling techniques are now able to handle them correctly in the right environment.

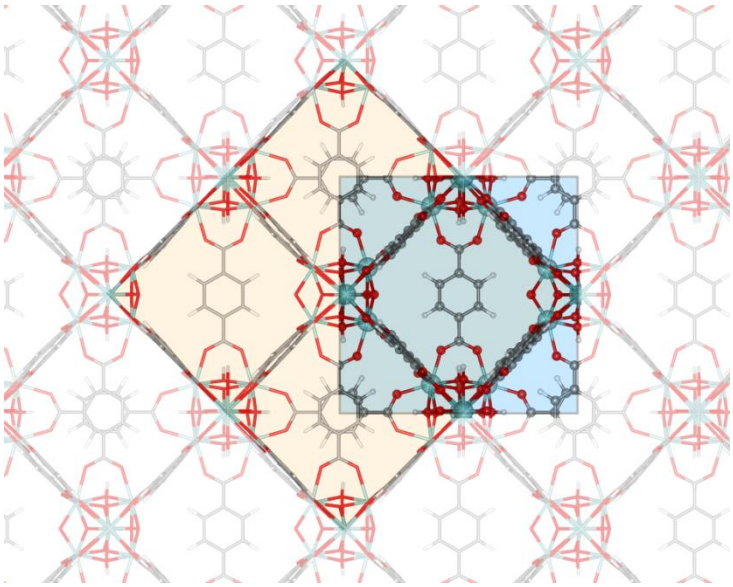

Figure 6: Conventional unit cell of UiO-66 with two linker defects : $<Zr_6O_6(OH)_2(RCOO)_{10}>_2$ $<Zr_6O_4OH_4(RCOO)_{12}>_2$. For computational feasibility a unit cell with only two Zr-bricks is frequently used, as indicated in blue.

Summarizing, **modeling a chemical reaction in the pores of a zeolite** has been performed by several groups using the most advanced methods. The current tool box delivers all required techniques to model the catalytic site in a correct way. We don't find the same activity in literature **to model catalytic reactions in MOFs**. We think that there is no reason anymore to show any reluctance to handle MOFs in a first principles periodic model taking into consideration all features appropriate to MOFs, like the flexibility of the frame which is more pronounced than in zeolitic structures. However it will probably take several years in order to apply such advanced models on these challenging systems in a mainstream way.

3. General characteristics of a heterogeneous catalyzed reaction

Prior to reaction on a heterogeneous catalyst, at least one of the reactants has to adsorb at the active site. Thus, before being able to model a reaction – or to determine a reaction path along a well-defined reaction coordinate – dedicated simulations are needed to elucidate the characteristics of the adsorption complexes from which the reaction starts. These calculations also yield information on the surface coverage, which is important information when comparing theoretical data with experimental kinetic measurements. Indeed, the reaction rate depends on the fractional coverage of active sites by the reactants. A schematic illustration of the reaction profile for a typical zeolite-catalyzed reaction is shown in **Figure 7**. In particular, **Figure 7** displays the reaction profile for propene methylation on an acidic zeolite which is an important reaction step in the Methanol-to-Olefin (MTO) process. Experimentally, one measures the apparent activation energy (denoted as $\Delta E^{\ddagger}_{app}$ in **Figure 7**). From **Figure 7** it becomes clear that it is crucial to obtain proper adsorption data of reactants from a computational perspective to enable the direct comparison of theoretical rate constants with experimental data. As such, the experimentally measured apparent activation energies and reaction rates should not be compared with the calculated intrinsic barriers and rates but with apparent kinetic data.

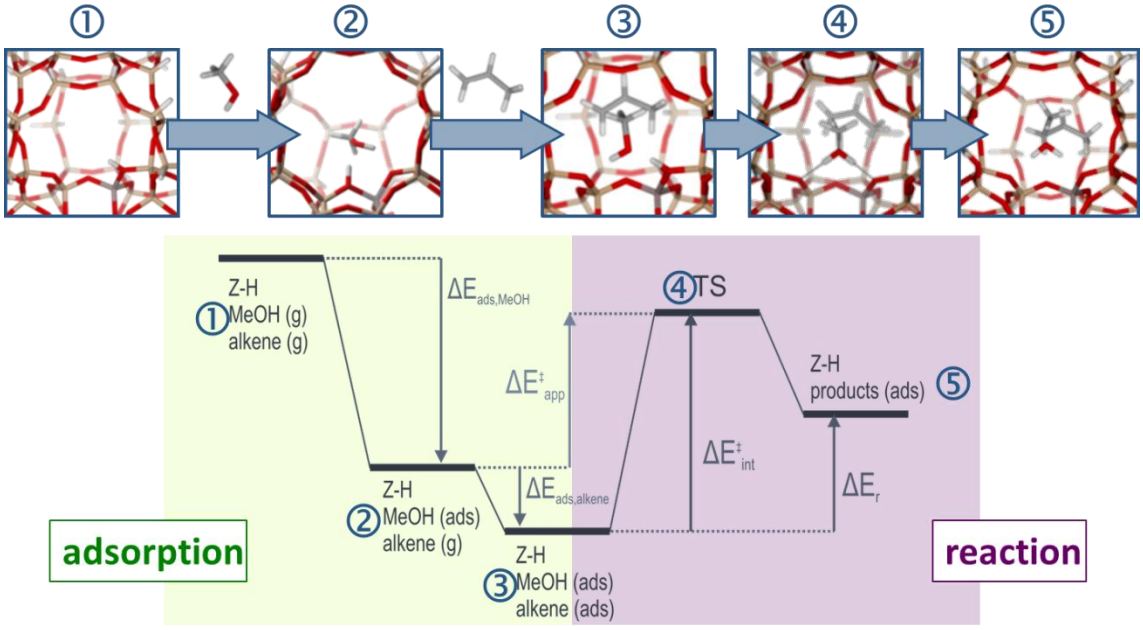

Figure 7: Schematic reaction profile of propene methylation over an acidic zeolite catalyst with indication of adsorption and reaction steps.

3.1 Determining critical points along the reaction pathway: Adsorption

As described above, an accurate description of adsorption in nanoporous materials is mandatory during the process of modeling heterogeneously catalyzed reactions. Various critical points along the reaction profile need to be determined theoretically and this can be done using a variety of theoretical models. As discussed in the previous section the modeler first needs to decide on the way in which the catalyst itself will be described, i.e. cluster/periodic. Once this choice is made, a next decision concerns whether the reaction profile will be modeled using static methods or methods that allow sampling of larger portions of the potential energy surface (PES). Static methods refer to techniques that only consider a limited number of points on the potential energy surface. In case of the previous reaction profile regarding propene methylation over an acidic zeolite catalyst (**Figure 7**), five states need to be described. The advantage of static approaches consists in its simplicity as only a limited number of points are necessary and these can be described with a high accuracy. However for some catalytic processes this approach clearly fails as one can simply not identify one reactant state. Moreover the structure/appearance/stability of intermediates is also sensitive to the operating conditions such as reaction temperature and pressure. In static methods the stability of intermediates at finite temperature is based on properties of the potential energy surface at 0 K. In order to clarify this item, we illustrate the advantage/disadvantage of static methods to describe the adsorbed state of the reactants.

A good example concerns the adsorption of alkenes in zeolites, which is a very challenging case both for theoreticians as for experimentalists due to the high reactivity of the intermediates even at low temperatures. When an alkene adsorbs on a Brønsted acid zeolite, various adsorbed species may be distinguished as schematically indicated in **Figure 8**. [66-69] A first state corresponds to a free alkene in the cages of the zeolite, which undergoes only a weak van der Waals (vdW) interaction with the walls of the zeolite. This state is further referred to as the physisorbed state. A more bound state corresponds to the π-complex, where a specific non-bonded interaction between the π-electrons of the double bond and the Brønsted acid site occurs. Finally the π-complex may be protonated leading to the formation of a chemisorbed species. [66-69] The nature of the resulting intermediate is still debated. It has been proposed to be stabilized as a covalently bonded alkoxide or as an ion pair which is referred to as a free carbenium ion (**Figure 8**). [33, 66, 67, 70, 71]

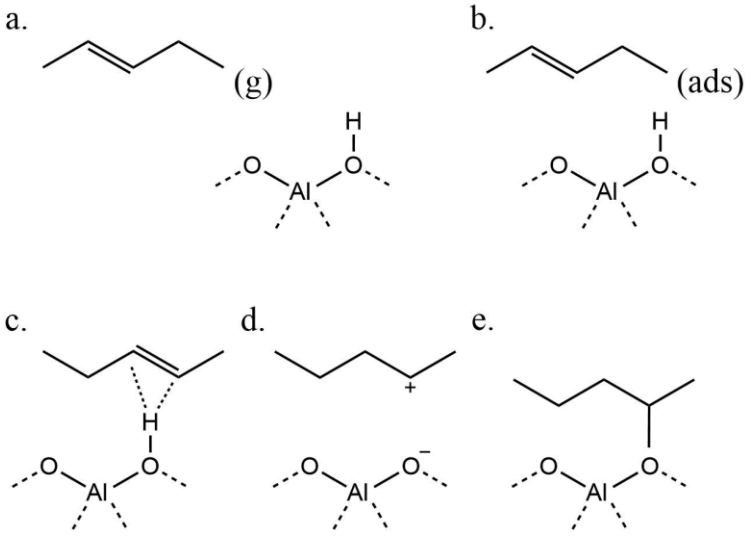

Figure 8: Illustration of the different intermediates upon alkene (2-pentene) adsorption in the presence of a Brønsted acid site (BAS): (a) alkene in gas phase, (b) alkene physisorbed in the

channels of the zeolite (c) alkene π-complex, (d) chemisorbed carbenium ion (e) chemisorbed alkoxide.

Solely based on experiment it is practically excluded to gain insight into the nature of the adsorbed complexes and intermediates, which can be very short-lived. Thus modeling may be an ideal complement to get track of these adsorbed species. However in this case we are confronted with a rather mobile molecule in the pores of the zeolite and it is very difficult to pinpoint one specific minimum on the PES at 0 K. In reality the PES is very flat yielding a multitude of almost isoenergetic minima. To deal with this complexity, one might sample the phase space with more advanced methods such as molecular dynamics (MD) methods. An extra assett of these methods is that they allow to take into account the flexibility of the material at realistic conditions of temperature or pressure. Depending on the statistical ensemble chosen during the simulation, i.e. NVT or NPT ensembles, one samples the system either under fixed conditions of cell volume and temperature or pressure and temperature. A more detailed explanation on statistical mechanics can be found in the reference work of Daan Frenkel and Berend Smit.[72] However it needs to be mentioned that excessively long simulation times are necessary to obtain statistically relevant average ensembles. Taken into account that these exercises are best done using high level quantum mechanical based methods, it is easily understood that such approach can not be regarded yet as the method of choice for daily applications. In case of pentene adsorption in H-ZSM-5, we determined probability distributions of some critical distances in molecular dynamics simulations of π-complexes and alkoxides in H-ZSM-5 obtained over a 60 ps run. The resulting probability distribution is shown in **Figure 9**.

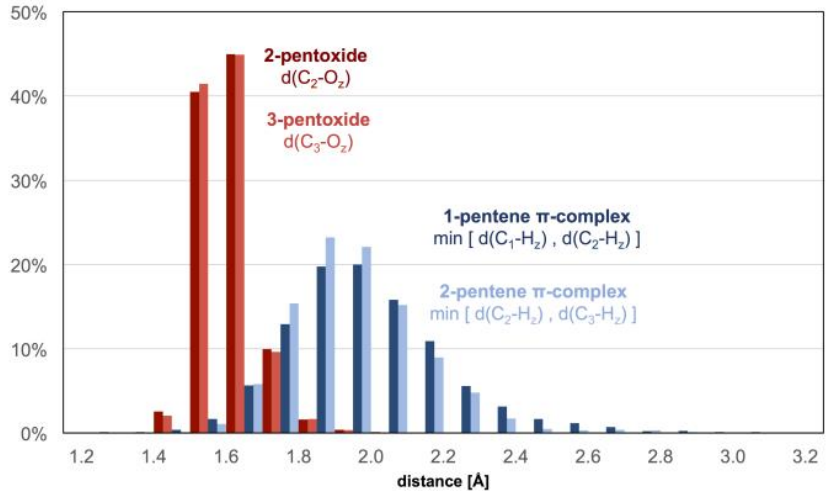

Figure 9: Probability distributions of some critical distances in molecular dynamics simulations of π-complexes and alkoxides in H-ZSM-5 obtained over a 60 ps run. Min[d(C_1-H_z),d(C_2-H_z)] stands for the shortest C-H_z distance in 1-pentene π-complex [average 2.07 Å]; Min[d(C_2-H_z),d(C_3-H_z)] stands for the shortest distance in the 2-pentene π-complex [average : 2.04 Å]; d(C_2-O_z) is the C_2-O_z distance in 2-pentoxide complex [average: 1.62 Å]; and d(C_3-O_z) is the C_3-O_z distance in 3-pentoxide complex [average: 1.62 Å]. Reproduced from ref. [73] with permission of Elsevier.

The distribution of the 1-pentene π-complex is interesting as the distribution is rather asymmetric towards longer interaction distances of the alkene bond and the Brønsted acid site. This means that

at finite temperature the complex will on average be positioned slightly further away from the acid site than predicted from static calculations at 0 K. Furthermore various orientations of the alkene with respect to the acid site and the zeolite walls are accessible. To determine adsorption enthalpies from these simulations various methods can be applied. One can opt to select some frequently sampled structures from the MD simulation and perform static energy refinements on these complexes or one could deduce the adsorption enthalpies from the molecular dynamics simulations themselves. Strictly spoken this last procedure might be preferred, but our experience learns that excessively long simulation times are necessary to achieve converged values for the adsorption enthalpies. Furthermore the overall computational cost of an MD simulation is determined by the level of theory chosen to determine the energies and forces. At present ab-initio MD simulations based on DFT are mostly performed with gradient-corrected exchange-correlation functionals complemented with dispersion forces not involved in the DFT functionals. More advanced functionals or other high level electronic structure methods can certainly enhance the accuracy of the deduced adsorption enthalpies from MD simulations, but these calculations are very demanding and a reduction of the total simulation time to partly compensate for the huge computational time is not an optimal solution. More information on the level of theory is given in the next section of this chapter.

Previous discussion shows that the study of a complex chemical transformation ideally combines the advantages of static and dynamic approaches, as both methods have their merits and deliver complementary information.

The advantages of static approaches relate to the fact that most advanced levels of theory are available to describe the energies of the system. A good simulation of the adsorption of guest molecules inside the pores of a nanoporous material requires an accurate description of non-covalent interactions such as electrostatic, hydrogen bonding and van der Waals interactions between the guest molecules and the host material. Density functional theory (DFT) methods are the method of choice to treat large systems, as they offer a favourable balance between accuracy and computational efficiency. However, a general drawback of commonly applied local density functionals is that they cannot describe long-range electron-electron correlations that are responsible for the dispersion forces. The latter are in many works colloquially named van der Waals (vdW) forces. In most of the functionals the missing dispersion forces are added as correction terms, while in some contemporary DFT functionals attempts have been made to incorporate dispersion directly by inserting specific terms and by an appropriate parameterization of the functional parameters. A short discussion of the frequently used DFT levels of theory in recent works is presented in the next subsection.

Levels of theory (LOTs) in periodic codes:

Nowadays many codes are available, offering a plethora of theoretical techniques to study the energies of a periodic system. We can illustrate this point based on our experience with VASP calculations. The VASP package [62-65] is one of the major software codes available to perform calculations on periodic structures of framework materials using a whole scope of different levels of theory. [23, 35, 74, 75] As already mentioned gradient-corrected exchange-correlation functionals are largely preferred in geometry optimizations such like PBE,[76] BLYP and revPBE [77] with D3

corrections of Grimme [34] for the missing dispersion forces. While hybrid DFT functionals with exact exchange like B3LYP are currently implemented in VASP, they are systematically not used in the geometry optimization of the extended system but only at the final stage for energy refinements. The only plausible reason is the high computational cost for a hybrid functional which does not necessarily lead to better geometries of the complex consisting of a periodic nanoporous material and some guest molecules in the pores. There exists a general consensus that the plane wave kinetic energy cutoff may be not lower than 600 eV (for zeolites) and 500 eV (for MOFs) when applying the projector augmented approximation (PAW). The criterion for energy convergence may not be larger than 10^{-7} eV. Further, in literature there exists a lot of inconsistency whether or not the unit cell should be relaxed during the geometry optimization. Relaxation energies can easily rise up to 25 kJ/mol per unit cell, suggesting a consistent use of the optimization procedure in the entire cycle of calculations to avoid numerical inaccuracies which can rise to unphysical proportions when subtracting binding energies from each other as is the case for the computation of adsorption enthalpies.

While D3 is generally accepted to be a reliable correction scheme for dispersion, especially in combination with PBE and revPBE, other contemporary dispersion models are available and easily handled in the energy refinement procedures like BEEF-vdW,[78] PBE with the new many body dispersion (MBD) scheme of Tkatchenko with conventional (MBD-vdW-H) and iterative Hirschfeld partitioning (MBD-vdW-HI). [79, 80]

DFT is no longer the only feasible many-particle methodology in periodic codes, very recently other many-body perturbation methods like the random phase approximation (RPA) are implemented in the VASP code. RPA contains dynamic electron correlations combining long-range dispersive and short-range exchange effects by continuously changing from the Kohn-Sham Hamiltonian to the exact many-body electron-electron interaction.[81] The exchange-correlation energy can thus be extracted from the electronic response in an (in principle) exact way. Actually, the number of effective applications of RPA on periodic nanoporous materials is rather limited. We refer to a successful application on alkane adsorption in Na-exchanged chabazites.[82] In this work RPA outperforms by far DFT-based methods even with the most advanced exchange-correlation functionals. Highly accurate electronic-structure methods like RPA have not been applied so far on MOFs, although calculations are under way to improve the understanding of energetic and mechanical behavior of framework materials.

This brief overview shows that from a methodological point of view a plethora of methods are available to study reactions in periodic static models. The only obstacle for usage of computationally very expensive methods on a regular basis is the computer time and the large number of atoms one is often confronted with for realistic models (easily adding up to 500 atoms per unit cell in MOFs). Extended cluster models were quite often used in the past but lose their attractiveness in this matter as higher levels of theory don't compensate the lack of a correct description of the nanoporous environment.
While **static periodic calculations** can be performed at the highest level of theory, this is by far not the case in **molecular dynamics (MD) simulations**. This emphasizes the complementarity between the two approaches. The focus of MD is different, and the information gathered after a MD run can be captured as input for a static calculation at high LOT.

To illustrate the complementary features obtained from static and molecular dynamics simulations, a summarizing adsorption enthalpy diagram for various adsorbed complexes of pentene is given in **Figure 10**. Adsorption enthalpies obtained from static calculations at 0 K are systematically larger than dynamically averaged values, since only the optimized structure of the π-complex at 0 K is taken into account. Thermal fluctuations on the relative distance of the complex with the Brønsted acid site give a better representation of the dynamical adsorption process and give adsorption enthalpies which are on average 20-30 kJ/mol less stable compared to their static values. Static periodic calculations have the advantage that they allow to use a large variation of DFT functionals and dispersion models. Göltl et al. observed same features for the adsorption behavior of alkanes and proposed to dynamically weight statically obtained adsorption enthalpies. [34] Based on our observations this might indeed be a good practice for future adsorption studies.

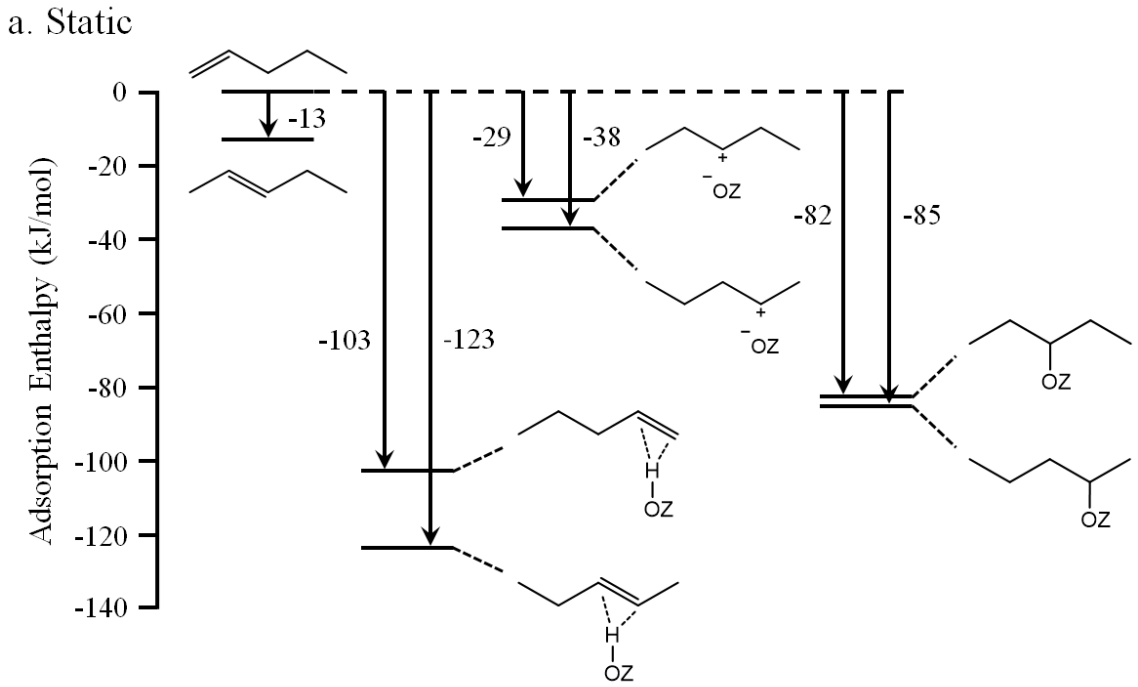

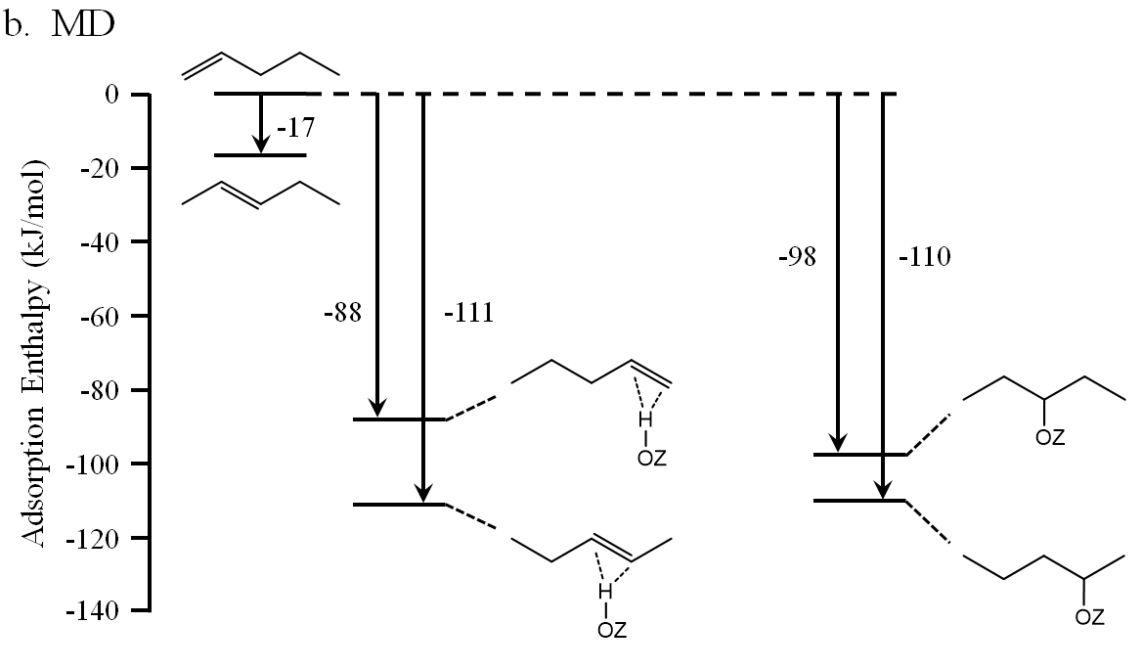

Figure 10: Adsorption enthalpy diagrams at 323 K for the several pentene intermediates with reference to 1-pentene in gas phase and an empty H-ZSM-5 framework obtained from (a) static calculations at the PBE-D3 level (b) MD simulations at the revPBE-D3 level. Reproduced from ref. [73] with permission of Elsevier.

3.2 Identifying transition state regions for complex chemical transformations

To finally study the chemical conversion itself, one needs to identify transition state regions. To this end, a reaction coordinate needs to be identified that leads the system smoothly from the reactant to the product region. It corresponds to that specific generalized coordinate for which maximum energy is reached during the transition from reactants to products. In its simplest form, the reaction coordinate corresponds to a single bond length or bond angle. For more complex reactions, however, the reaction coordinate is multidimensional and can only be approximated by a combination of bond lengths and/or bond angles, or even by non-geometric parameters such as bond orders or coordination numbers.

When studying chemical reactions with static methods, one needs to identify the transition state or activated complex, which is a minimum in all directions except for one coordinate that leads the system from the reactant to the product valley. To identify transition states, no single well-determined recipe is available and it needs a very experienced user to localize these critical points along the reaction path. Transition state optimization routines are still much better equipped in molecular based programs such a Gaussian [83] than in periodic solid state codes. Therefore one often opts to first localize critical points along the reaction path using extended cluster models and then import these geometries in periodic codes. An example of a transition state that was first localized in cluster based models and then transferred to periodic frameworks is shown in **Figure 11.** Herein**,** the unit cell of UiO-66 is displayed with one missing linker and a reactive complex with two adsorbed species: benzaldehyde and propanal. The figure gives an indication of the complexity of

the active site (encircled) and of the necessity to use the conventional unit cell of 4 Zr-bricks (orange cell in **Figure 6**), or the reduced cell with only two Zr-bricks (blue cell in **Figure 6**) as applied in **Figure 11**.

The transition state TS1 is part of a reaction pathway corresponding to the aldol condensation between benzaldehyde and propanal, which is taken as a model reaction for the condensation reaction to form the jasminaldehyde condensation product from benzaldehyde and heptanal. [56] Experimentally it was shown that under certain conditions, Zr-terephthalate MOFs (UiO-66) are highly selective catalysts for this cross-aldol condensation. However it was very difficult to propose the exact reaction mechanism. Therefore we performed Density Functional Theory (DFT) calculations on an extended cluster to elaborate on a plausible reaction pathway that is schematically shown in **Figure 11**. Once the whole aldol condensation reaction mechanism has been unraveled in the cluster approach, further refinement can be accomplished with periodic models accounting properly for the topology of the UiO-66 material. By way of illustration the free energy profile obtained with periodic models is also displayed in **Figure 12** allowing a comparative study with the cluster results. Qualitatively the main features of the reaction scheme are preserved, although quantitatively relatively large differences are found for the adsorption steps. For a more mechanistic discussion of the reaction – which is not the objective of this book chapter - the interested reader is referred to the original paper. [56]

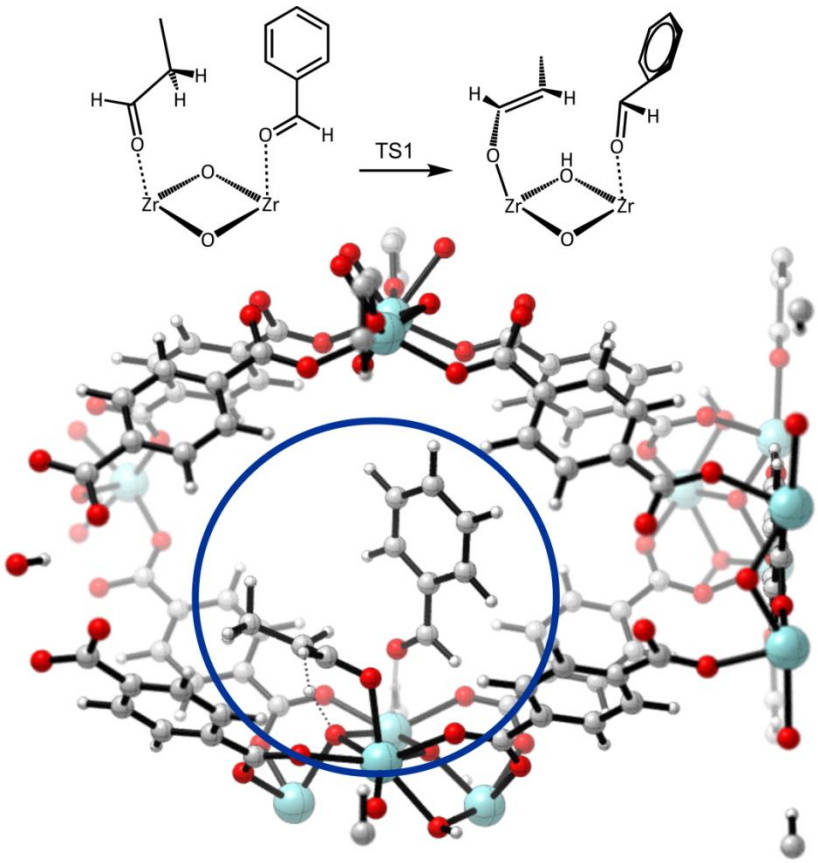

Figure 11: Adsorption of benzaldehyde and propanal at the Lewis acid site (Zr-atom) as a reactive complex before the aldol condensation. [56] As material we consider here UiO-66 with some linker defects to create an active site on a Zr-brick.

This is a typical example of a reaction where initial exploration of various transition states needs to be done in a computationally efficient way (use of extended cluster models) since a lot of intermediates and transition states are involved.

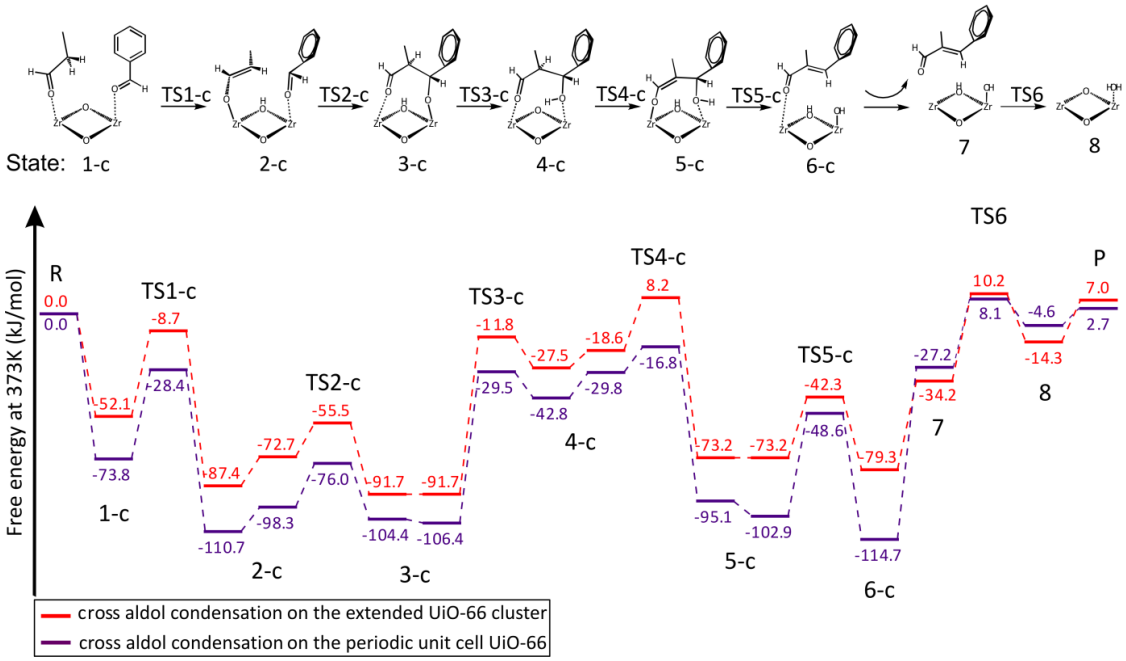

Figure 12: Schematic representation of the cross aldol condensation. Comparison of the free energy profiles between two models, cluster (red) and periodic (violet) UiO-66 for the jasminaldehyde condensation, calculated at 373 K. Level of theory on the cluster: B3LYP/6-311++G(d,p)-D3//B3LYP/6-31G(d)*. Level of theory on the periodic unit cell: B3LYP-D3(BJ)// PBE-D3(BJ). R corresponds to the reactants in gas phase and the cluster, P corresponds to the final product and water in gas phase and the cluster. Taken from ref. [56].

Summarizing, the periodic model, in which we account for the environment of surrounding linkers and other Zr Lewis acid sites, gives a more accurate description of the system. Although, the qualitative aspects of the mechanism are fairly well described by the extended cluster model.

A side note which is very relevant here concerns the validation of the correct transition states. This should be done using a normal mode analysis. A correct transition state should be characterized by all positive frequencies except for one coordinate which leads us along the reaction coordinate. Performing a normal mode analysis within periodic codes is very challenging, one often is confronted with small negative frequencies which are due to global modes of the system and the nature of the PES which may be very flat. It may be very time consuming to remove all of these low lying spurious frequencies, but in principle this elaborate work needs to be done to localize and identify the true transition state. Moreover, when it is the aim to calculate free energies and kinetic data it is of utmost importance that normal modes with low frequencies are properly described as they have a significant contribution to the vibrational partition function (vide infra). In literature we observe that some authors substitute these low lying frequencies artificially with some value varying between 12 and 30 cm^{-1} to perform the thermochemical analysis.

The previous example was a showcase example of a complex reaction due to many reaction steps and the complexity of the molecular environment. However in this case it was possible to identify proper transition states using static methods. In some cases it might be more difficult to use this methodology and one needs to use more advanced techniques that sample rather transition state regions instead of one single transition state. Hereafter we show some applications of these more advanced techniques in zeolite catalysis to illustrate the workflow one needs to follow in such case.

We consider the methylation reactions of aromatic species in zeolites with various topologies. The general reaction scheme is given in **Figure 13.**

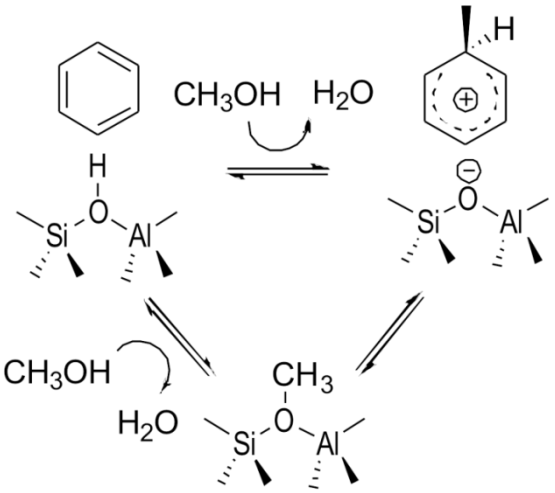

Figure 13: Schematic representation of the reaction mechanism of the zeolite-catalyzed methylation of aromatic species. Adapted from ref [11] with permission from Wiley.

The methylation reaction of benzene with methanol can occur via two pathways, a direct path in which the methyl group of the methanol is transferred in one step to the aromatic species or an indirect route in which first a methoxide species is formed playing the role of a methylating agent in the second step. It has been shown in literature that the two pathways might become competitive at certain operating conditions.[10, 84, 85]

In a first example we show some modeling results of this methylation reaction in H-ZSM-5 but at various loadings of methanol molecules. Indeed the standard way of studying this reaction accounts for only one methanol molecule, however at realistic operating conditions, more methanol molecules may be present in the pores of the zeolite and these may change the overall reactivity. This example is a typical case where static methods fail in describing the situation whereby more than one methanol molecule is in play. It is realistic to imagine that multiple geometries are present in the description of reactant complexes and transition states with nearly equal energy and that the concept of one single geometry fails as is standard in static approaches. It is a showcase example where molecular dynamics studies can offer an enormous added value compared to static methods.

Figure 14 shows the free energy profile for the concerted methylation of benzene in H-ZSM-5 with 5 methanol molecules with selected conformations representing four phases along the reaction pathway. It seems that prior to reaction methanol clusters can be present (phase I in **Figure 14**). The methanol that transfers its methyl group to the aromatic molecule then first has to escape the

cluster conformation (phase II) to be able to undergo the actual methylation reaction (phases III and IV). The identification of these 4 phases originates from the dynamical approach applied in this study.[13]

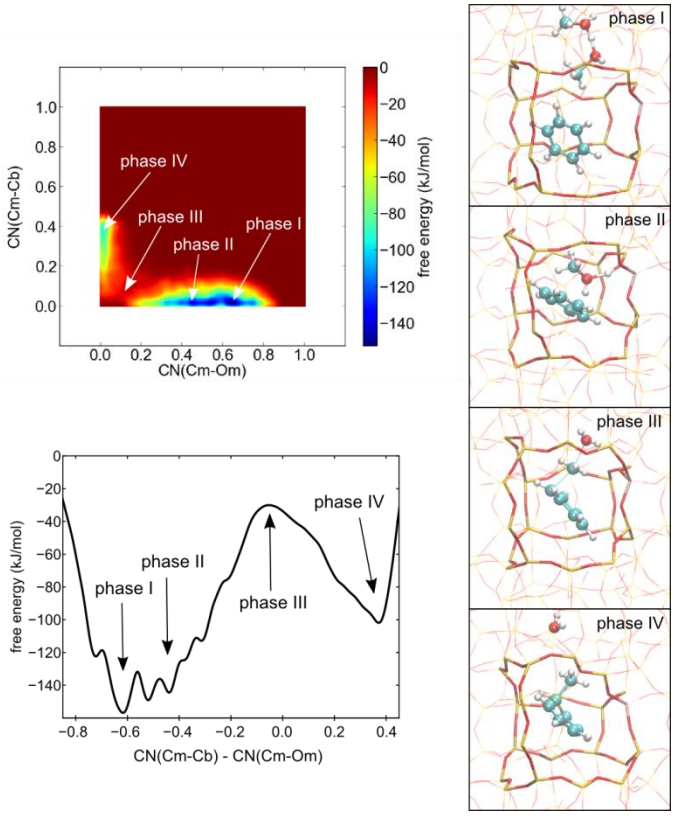

Figure 14: 2D (top left) and 1D (bottom left) free energy profile for the methylation of benzene in H-ZSM-5 with 5 methanol molecules with selected conformations representing the four phases along the reaction pathway (shown right). Methanol molecules that do not participate in the reaction are not shown. Reproduced from ref. [13] with permission of the American Chemical Society.

It should be noted that, in order to study reactions with a dynamical approach, regular MD simulations are mostly not able to sample transition state regions. Indeed, chemical transformations are rare events as their probability of occurence is very low, although once it occurs the event may be followed during a regular MD run of a few picoseconds. To enhance sampling of interesting regions of the free energy surface a multitude of methods has been developed. [23] The example shown above has been performed using the **metadynamics (MTD) a**pproach developed by Laio and Parrinello.[86, 87] The concept of such metadynamics approach is illustrated in **Figure 15**. It relies on the choice of a limited number of collective variables along which the free energy landscape is filled up with Gaussian hills to accelerate sampling of events. Afterwards the sum of the Gaussians defines a bias potential for the simulations which can be used to reconstruct the free energy surface. To date the method is well developed and implemented in a series of computer packages such as CP2K, CHARMM, …. The usage however of the method for applications in nanoporous materials is rather limited. The practical execution requires special skills from the user, which are not available in a toolbox. For reactions occurring in the pores of a zeolite the MTD methodology has been applied for the first time by Moors et al. [13] and more recently by De Wispelaere et al.[10, 12, 75]

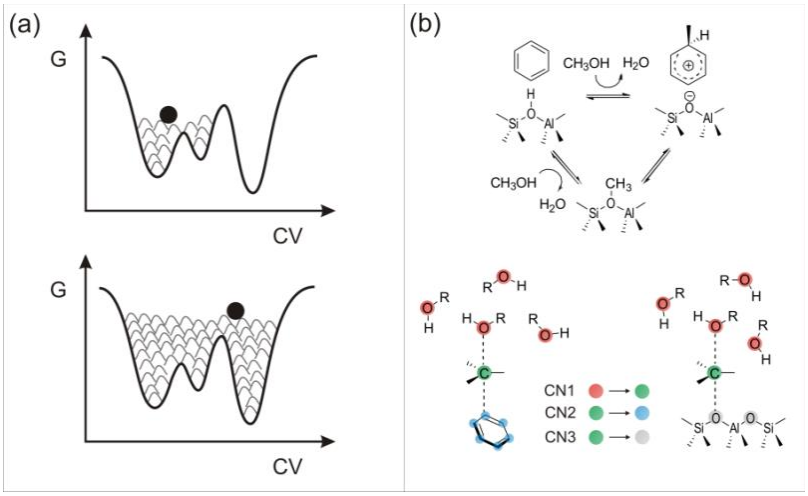

Figure 15: Gaussian hills construct the bias potential during a metadynamics run (a). To describe competing reaction paths, a high number of atoms should be included in the collective variables as illustrated for a methylation pathway (b)

As described above, a dynamical approach is beneficial in cases where multiple guest molecules make the reaction environment more complex. Another important example is when broad reactant state and transition state regions can be expected. To illustrate this we again consider the methylation of benzene by methanol, but this time in the large pore zeolite H-SSZ-24. Due to its unidirectional 12-ring channel, this material gives a lot of configurational freedom to the guest molecules at high temperature (623 K in this case).[11] With the metadynamics approach a plethora of geometrically inequivalent and nearly isoenergetic transition states have been sampled as can be seen in **Figure 16**. It is obvious that all these configurations have an impact on the calculated free energy barriers and kinetic data for this reaction. Moreover, in this work the concerted and stepwise methylation reaction (cfr. **Figure 13**) have been sampled in one single run in order to explicitly account for the potential competition of both reaction mechanisms at elevated temperature. It was indeed confirmed that both reaction pathways exhibit nearly identical free energy barriers under these conditions.

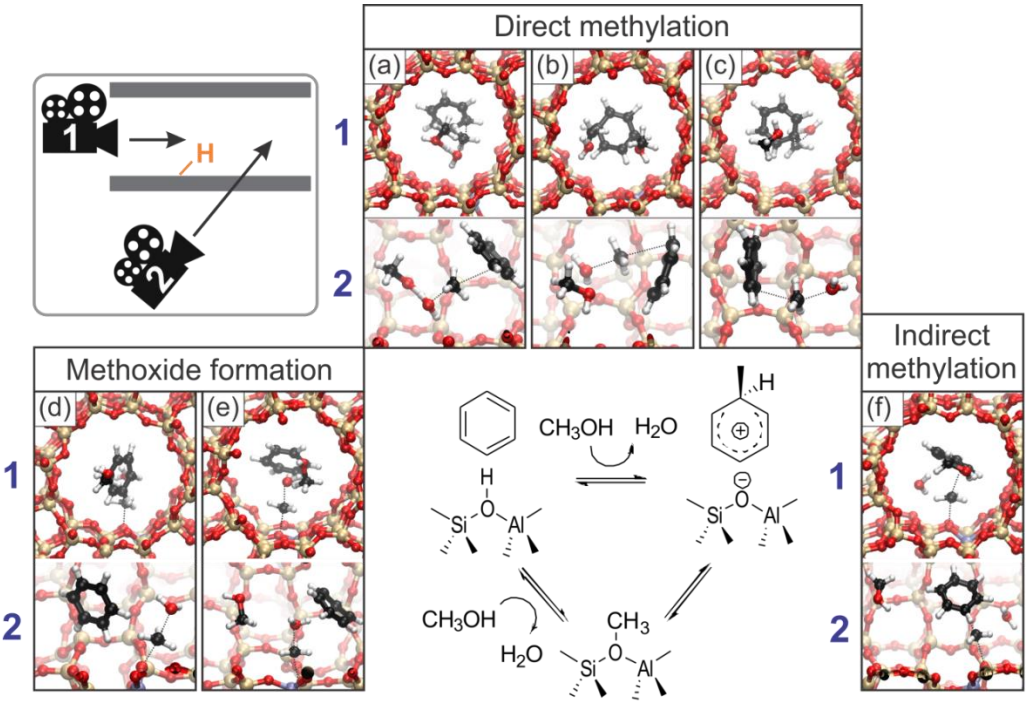

Figure 16: Snapshots of the concerted (a,b,c) and stepwise methylation (d,e,f) of benzene by 2 methanol molecules in H-SSZ-24 at 623 K, seen in the direction of the 1D channel (camera viewpoint 1) and in a cross section of the channel (camera viewpoint 2).

The success of MTD critically relies on a proper choice of the collective variables which enable us to walk on a privileged minimum energy path on the free energy surface, but MTD has also its limitations. MTD requires some prior knowledge of the reaction mechanism, but as a result of this knowledge one introduces some bias in the multiple constraints imposed during an MTD run. Another issue concerns the accuracy one may obtain using metadynamics methods. To our opinion some dedicated benchmark studies are necessary to validate the method for well-studied reactions in zeolite catalysis. Such studies are underway.

Among other advanced MD techniques without prior knowledge or specification of transition states belongs transition path sampling which combines Monte Carlo moves on MD trajectories.[88, 89] Hereby reaction paths or trajectories are generated between reactant and product valley (see **Figure 17**). By means of perturbations on an initial trajectory between R and P one creates new paths and thus finally one disposes of an ensemble of transition paths. From the dynamics of each path in the ensemble an ensemble averaged reaction rate coefficient can be determined.[89] This method has shown to be very successful especially in the modeling of zeolite catalyzed reactions as demonstrated by Bučko et al. [90]

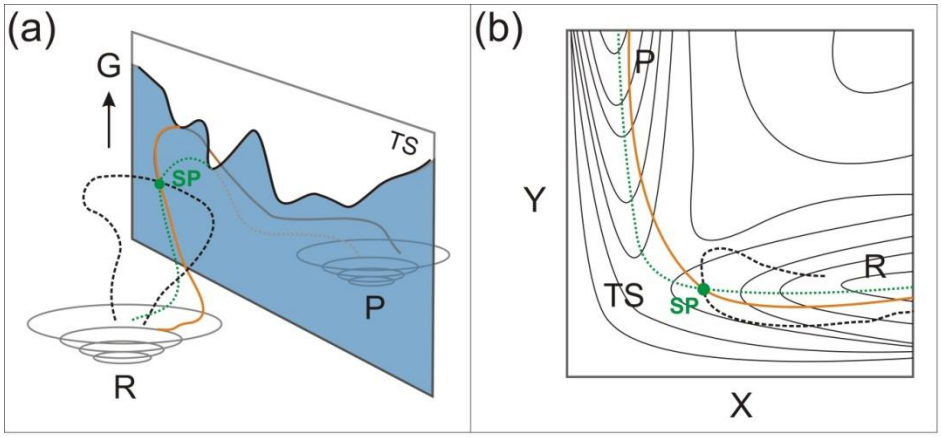

Figure 17: Schematic representation of the free energy landscape with two stable wells separated by a transition state ridge (a). From the initial path (full orange line) a new reactive trajectory (green dotted line) is shot from shooting point SP. The black dashed line represents a non-reactive trajectory (a). Part (b) shows the same trajectories on contours of a potential energy surface. Adapted from ref. [91] with permission from the Royal Society of Chemistry.

4. First principle chemical kinetics from static and dynamic calculations

The determination of rate constants of elementary chemical reactions taking place in nanoporous materials from first principles has reached such a level of accuracy that molecular control over production processes (yield, selectivity, etc.) by theory is achievable. A lot of theoretical papers within zeolite and MOF catalysis primarily focus on various mechanistic aspects of the catalytic reactions. Herein reaction barriers play an essential role.

Key property of chemical kinetics and the determination of the rate constant is the Gibbs free energy barrier which differs in its computation in static and dynamic calculations. In the latter a large number of states is sampled, and an averaging over all samples yields quantities which satisfy statistical grounds provided phase space is sufficiently sampled during the dynamic simulation. This methodology is the only correct procedure if sufficiently large simulation times are respected. Currently the explosive expansion of computer capabilities enables the performance of such large simulations on extended and complex systems, but it is clear that this procedure is not appropriate as standard method of choice for any catalytic reaction taking place in the pores of a nanoporous material. In most of the cases one falls back to the reproduction of the three stationary points, which initial structures are inspired by the various reaction paths suggested in the MD simulations.

Static approach – Transition State Theory (TST): Within the static approach the reaction is described by three stationary points : reactive complex , TS and the product complex. All stationary points are determined at 0 K. For most catalytic reactions in the pores of a nanoporous material the PES is very flat and multiple reactive complexes- differing with some few kJ/mol – are valuable candidates as reactant in the static approach of the reaction. As outlined in previous sections standard AIMD simulations can assist in extracting suitable initial structures for the geometry optimization of the adsorbed complexes. Important issue is that a static optimization reflects the situation at 0 K, with the consequence that the found equilibrium distances characterizing the

reactant complex do not correspond with the real situation which takes place at finite temperatures. This shortcoming can lead to over- or underestimation of reaction barriers, and thus a serious shortcoming of the static approach. The further procedure in a static approach consists in evaluating the partition functions from the frequencies belonging to the geometries of the three stationary points. Note that the transition state or activated complex represents a saddle point on the multidimensional potential energy surface, i.e. minimum in all degrees of freedom except in the reaction coordinate for which a maximum is reached.

The reaction rate constant is given by $k(T) = \frac{k_B T}{h} V^{-\Delta^{\ddagger} n} e^{-\frac{\Delta^{\ddagger} G}{RT}} = \frac{k_B T}{h} V^{-\Delta^{\ddagger} n} e^{\frac{\Delta^{\ddagger} S}{R}} e^{-\frac{\Delta^{\ddagger} H}{RT}}$ (1)

In this expression k_B represents the Boltzmann constant, T stands for the temperature, h is Planck's constant and R is the universal gas constant.

For a **unimolecular reaction** $\Delta^{\ddagger} n = 0$ and the rate constant $k(T) = \frac{k_B T}{h} e^{-\frac{\Delta^{\ddagger} G}{RT}}$ is expressed in s^{-1}.

For a **bimolecular reaction** A + B -> $(AB)^{\ddagger}$ ($\Delta^{\ddagger} X = X_{AB^{\ddagger}} - X_A - X_B$) is $\Delta^{\ddagger} n = -1$ and the rate constant $k(T) = \frac{k_B T}{h} V e^{-\frac{\Delta^{\ddagger} G}{RT}}$ is expressed in units $dm^3\ mol^{-1} s^{-1}$.

It is common to decompose the free energy of activation into the standard enthalpy of activation and the standard entropy of activation, following

$$\Delta^{\ddagger} G = \Delta^{\ddagger} H - T\Delta^{\ddagger} S \quad (2)$$

with

$$\Delta^{\ddagger} H = \Delta^{\ddagger} U_0 + \Delta^{\ddagger} U_{therm} + RT\Delta^{\ddagger} n$$
$$= \Delta^{\ddagger} U + RT\Delta^{\ddagger} n$$

and thus

$$\Delta^{\ddagger} H = \Delta^{\ddagger} U - RT \quad (3)$$

for a bimolecular reaction as for a reaction of a gas with active site on a solid surface , and

$$\Delta^{\ddagger} S = R \ln\left(\frac{Q^{\ddagger}}{Q_A Q_B}\right) + \frac{1}{T}\Delta^{\ddagger} U_{therm} \quad (4)$$

In case of a bimolecular reaction in which one of the reactants represents a fixed framework (e.g. chemisorbed complex), that reactant does not contain translational nor rotational degrees of freedom.

We refer to the appendix for some thermodynamic expressions elucidating the above discussion.

The static frequency calculations for the two stationary states (pre-reactive complex and TS for the forward reaction) lead to the direct computation of :

- the electronic barrier ΔE_0 including zero point energies (ZPE) from the various vibrational modes :

$$\Delta^{\ddagger} U_0 = \Delta E_0 = E_0^{\ddagger} - E_0^A - E_0^B + \Delta E_{0,vib}$$

with

$$\Delta E_{0,vib} = \sum_{i=1}^{N^{\ddagger}} \frac{1}{2} h\nu_i^{\ddagger} - \sum_{i=1}^{N_A} \frac{1}{2} h\nu_i^A - \sum_{i=1}^{N_B} \frac{1}{2} h\nu_i^B$$

- the partition functions $\left(\frac{Q^{\ddagger}}{Q_A Q_B}\right)$ defining the entropy of activation.

- the small thermal corrections $\Delta^{\ddagger}U_{therm}$ which are also determined from the frequencies (see Appendix).

Partition functions are unit less quantities, and thus also $\left(\frac{Q^{\ddagger}}{Q_A Q_B}\right)$ but its evaluation requires the value of the volume V by means of the translational partition functions. A further elucidation is obtained by factorizing the expression of the partition functions into translational and other degrees of freedom :

$$\left(\frac{Q^{\ddagger}}{Q_A Q_B}\right)=\left(\frac{Q^{\ddagger}}{Q_A Q_B}\right)_{trans}\left(\frac{Q^{\ddagger}}{Q_A Q_B}\right)_{other}=\left(2\pi\frac{m_A m_B}{m_A+m_B}k_B T\right)^{-3/2}\frac{h^3}{V}\left(\frac{Q^{\ddagger}}{Q_A Q_B}\right)_{other}$$

The reaction rate constant can then be expressed in the form :

$$k(T)=\frac{k_B T}{h}\left(2\pi\frac{m_A m_B}{m_A+m_B}k_B T\right)^{-3/2}h^3\left(\frac{Q^{\ddagger}}{Q_A Q_B}\right)_{other}e^{-\frac{\Delta E_0}{RT}},$$

which clearly illustrates the V-independence of k(T) but involving the correct dimension of s^{-1}. dm^3 or s^{-1}. m^3. By multiplying with the number of Avogrado N_A the bimolecular rate constant k(T) can be expressed in units s^{-1} dm^3/mol as usual.

Dynamic approach :
Standard ab initio MD simulations are frequently used to explore the whole phase space and to attain an almost complete sampling of the conformational space. This is of particular use in the exploration of the plausible complexes of reactants adsorbed to the active site of the catalyst.

Most often sufficiently long NVT simulations are run and they deliver ensemble averages of the internal energies obtained by averaging the sum of potential and kinetic energy. This procedure allows us to determine the adsorption energy for the adsorbed complex of reactant molecules by performing separate NVT runs on the complex, the empty nanoporous material (zeolite, MOF) and the adsorbate in gas phase:

$\Delta U_{ads} = \langle E_{complex}\rangle - \langle E_{nanoporous}\rangle - \langle E_{reactants}\rangle$ (5)

The corresponding adsorption enthalpies are then given by

$\Delta H_{ads} = \Delta U_{ads} - RT$ (6)

in which R is the universal gas constant (at 323 K: RT = 2.7 kJ/mol).

As mentioned earlier regular MD simulations cannot efficiently sample catalytic reactions for potential energy surfaces where the basins are separated by relatively high potential ridges. In this case advanced MD techniques are here required to enhance the occurrence of the rare event. They all incorporate constraints to guide the complex systems during the simulation along the desired reaction path. By these constraints the MD runs does not explore the complete potential energy surface anymore but rather a region around the minimum-energy path.

Constrained MD simulations give access to free energy profiles of chemical processes. By means of Eq.(1) rate constants may eventually be extracted. However, this implies that the free energy of activation should result from the simulations.

The MTD approach relies on the selection of a set of collective variables that describe the reaction under study. This often leads to multidimensional free energy surfaces which are complex to interpret and from which it is difficult to extract a free energy barrier. We illustrate the approach to extract a free energy barrier based on a free energy surface for an MTD simulation with two collective variables which yields a 2D free energy surface. First, the 2D free energy surface can be projected onto a 1D profile according to:

$$G(CV2-CV1) = -\frac{1}{k_B T}\ln\left\{\int_{-\infty}^{+\infty} d_{CV1}\exp[-\frac{1}{k_B T}G(CV2-CV1,CV1)\right\} \quad (7)$$

Alternatively one can calculate the lowest free energy path (LFEP) on the calculated FES as described by Ensing et al.[11, 92]

Based on the one-dimensional free energy profile it is now essential to calculate the free energy for each state, i.e. for the reactants, transition state region and product state.
In Appendix B a brief summary of elementary concepts of statistical physics is given, which assists the reader in understanding the correct post-analysis of a MTD run.

Suppose that at the end of a MTD simulation we are able to deduce a 1D free energy profile $G_q(s)$ as function of a collective variable *s*. Free energy and partition function of a microstate q are related with the expression:

$$G_q(s) = -k_B T \ln Z_q(s) \quad (8)$$

One could define a **macrostate A** for which s lies in the range [s_1, s_2]. This gives rise to the following expressions:

$$Z_A = \int_{s_1}^{s_2} Z_q(s)ds \quad (9)$$

$$G_A = -k_B T \ln Z_A = -k_B T \ln \frac{Z_A}{Z} - k_B T \ln Z \quad (10)$$

In this case Z_A, must be interpreted as the contribution to the partition function from the macrostate A. Similarly G_A can be interpreted as the free energy associated with the macrostate A which can be computed up to a constant G, which is the total free energy.

A more rigorous approach consists of dividing the complete range for s into three regions:

- the reactant region **R**=]-∞,s_0],
- the transition state region **TS** =[s_0, s_1] and

- the product region **P** = [s_1, +∞[.

This partition can easily be extended if the trajectory encounters more than 1 TS.

Now we can compute:

$$Z_R = \int_{-\infty}^{s_0} Z_q(s)\,\Delta s\,\frac{ds}{\Delta s} = \int_{-\infty}^{s_0} e^{-\beta G_q(s)}\,\Delta s\,\frac{ds}{\Delta s}\ ;\ G_R = -k_B T \ln Z_R = -k_B T \ln \int_{-\infty}^{s_0} e^{-\beta G_q(s)}\,\Delta s\,\frac{ds}{\Delta s} \qquad (11)$$

$$Z_{TS} = \int_{s_0}^{s_1} Z_q(s)\,\Delta s\,\frac{ds}{\Delta s} = \int_{s_0}^{s_1} e^{-\beta G_q(s)}\,\Delta s\,\frac{ds}{\Delta s}\ ;\ G_{TS} = -k_B T \ln Z_{TS} = -k_B T \ln \int_{s_0}^{s1} e^{-\beta G_q(s)}\,\Delta s\,\frac{ds}{\Delta s} \qquad (12)$$

$$Z_P = \int_{s_1}^{+\infty} Z_q(s)\,\Delta s\,\frac{ds}{\Delta s} = \int_{s_1}^{+\infty} e^{-\beta G_q(s)}\,\Delta s\,\frac{ds}{\Delta s}\ ;\ G_P = -k_B T \ln Z_P = -k_B T \ln \int_{s_1}^{+\infty} e^{-\beta G_q(s)}\,\Delta s\,\frac{ds}{\Delta s} \qquad (13)$$

To circumvent the dimensionality conflict here, we introduced Δs and defined $Z_q(s)\,\Delta s = e^{-\beta G_q(s)}$, which is inspired by the equation $G_A = -k_B T \ln Z_q(\bar{s})\,\Delta s$.

Having introduced free energies to each region, we are now able to define free energies of activation $\Delta G^{\ddagger}$ as :

$$\Delta G^{\ddagger} = G_{TS} - G_R = -k_B T \ln \frac{\int_{s_0}^{s_1} e^{-\beta G_q(s)}\,ds}{\int_{-\infty}^{s_0} e^{-\beta G_q(s)}\,ds} \qquad (14)$$

and reaction free energies ΔG_r :

$$\Delta G_r = G_P - G_R = -k_B T \ln \frac{\int_{s_1}^{+\infty} e^{-\beta G_q(s)}\,ds}{\int_{-\infty}^{s_0} e^{-\beta G_q(s)}\,ds} \qquad (15)$$

Δs drops out of the equation, so it does not influence the results.

The width of the TS region (s_0, s_1) is determined by the thermal fluctuation, which is given by the standard deviation of the collective variable s. We have systematically taken a value of 0.04, which represents the average of the thermal fluctuations measured at the local minima of the reactant valley.

From this discussion it becomes clear that more complex models – for example by applying a dynamical approach – also significantly increase the difficulty of data analysis. However, for some specific cases a dynamical approach seems mandatory to better mimic true reaction conditions.

5. Complementary insights from computational Spectroscopy

Apart from modeling the reaction itself, computational spectroscopy has evolved as an indispensable characterization tool to identify intermediates during a reaction. In-situ experiments deliver data which evolve in time, which vary with temperature and other operating conditions.[93] Infrared (IR), NMR spectra and other optical spectroscopic techniques are continuously recorded and give crucial information on the reaction intermediates which have been formed in function of time, under condition that these experimental spectra are correctly interpreted. This indispensable tool box is nowadays available due to the latest advances in the computation of the spectroscopic signals. It is not surprising that the most successful reproduction of spectroscopic spectra under real operating conditions come from molecular dynamics simulations.

Infrared (IR) spectroscopy is one of the leading characterization tools in zeolite and MOF chemistry covering the whole frequency range from low collective modes around 10 cm^{-1} to high frequency modes of bond stretches of about 4000 cm^{-1}. Vibrational frequencies of the eigenmodes of the system can be computed by construction of the Hessian matrix with the evaluation of the second order derivatives of the total energy with respect to Cartesian displacements of the atoms in the system. In a static periodic calculation such a frequency calculation with 400 or more atoms is not a trivial task and needs some practical skills to construct an optimized unit cell of the catalyst (with and without adsorbed reactant molecules) with all positive frequencies. Not all current computational works apply the correct procedure in eliminating in an adequate way the appearing imaginary frequencies. They prefer a pragmatic approach by replacing each imaginary frequency by a low positive frequency (this value can vary from 12 to 30 cm^{-1}). [94, 95] It should be stressed that this procedure generates large errors as low frequencies largely affect the vibrational partition functions leading to unphysical predictions for adsorption entropies and free energies. A static approach has further the disadvantage that all vibrations of the complex catalyst are treated within the harmonic approximation. Experimental vibrational and IR spectra are largely affected by anharmonicities and while they can also be incorporated in static approaches via non-trivial interventions, [96] they are best taken into account in molecular dynamics simulations where anharmonicities of the modes appear in a natural way. But MD on such complex systems are confronted with a serious obstacle that long simulations are practically not feasible, at least when ab initio MD (AIMD) simulations are concerned. A valid alternative could be the use of classical force fields which are developed for the material under investigation.

From the data recorded during the MD simulations infrared spectra can be obtained via the Fourier transformation of the dipole moment auto-correlation function $\langle d\bar{\mu}(0), \mu(t) \rangle$ leading to an expression for the IR adsorption cross section [97] : $\alpha(\omega) \sim \lim_{\tau \to \infty} \frac{1}{\tau} \left| \int_0^{\tau} dt\, e^{-i\omega t} \frac{d\bar{\mu}(t)}{dt} \right|^2$

As the time derivative of the dipole moment can be approximated as : $\frac{d\bar{\mu}(t)}{dt} = \sum_{i=1}^{N} q_i \bar{v}_i(t)$ with q_i the charge and v_i the velocity of atom i , a simple velocity power spectrum (VPS) offers an adequate theoretical tool to construct a potential IR spectrum. In a comparative study with experiment focus lies into the position of the peaks rather than the intensities of the peaks.

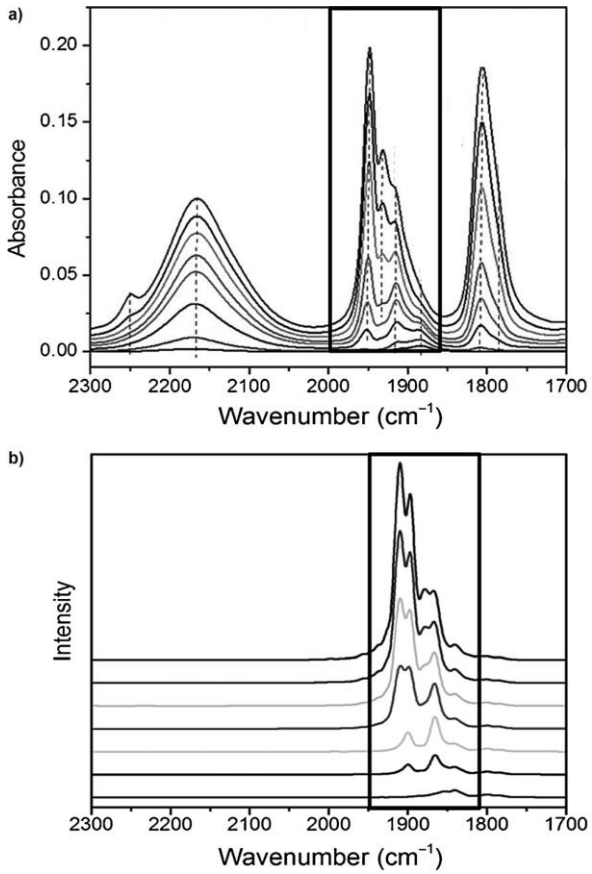

Figure 18. a) Experimental [98] and b) simulated IR spectrum [99] for different NO loadings adsorbed to copper(II) sites in zeolites . The modeled spectrum is based upon a linear combination of IR spectra corresponding with sites differing in the position of the Al substitution and of the Cu^{II} cation, and the Si/Al ratio. Taken with permission from ref. [99]

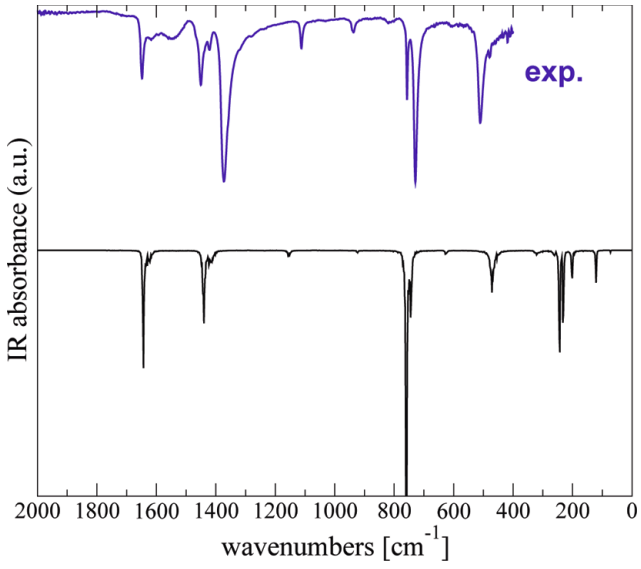

Figure 19: Comparison of the computed IR spectrum (bottom) with the measured (top) spectrum for a desolvated, activated Cu-btc sample. Taken from ref. [100]

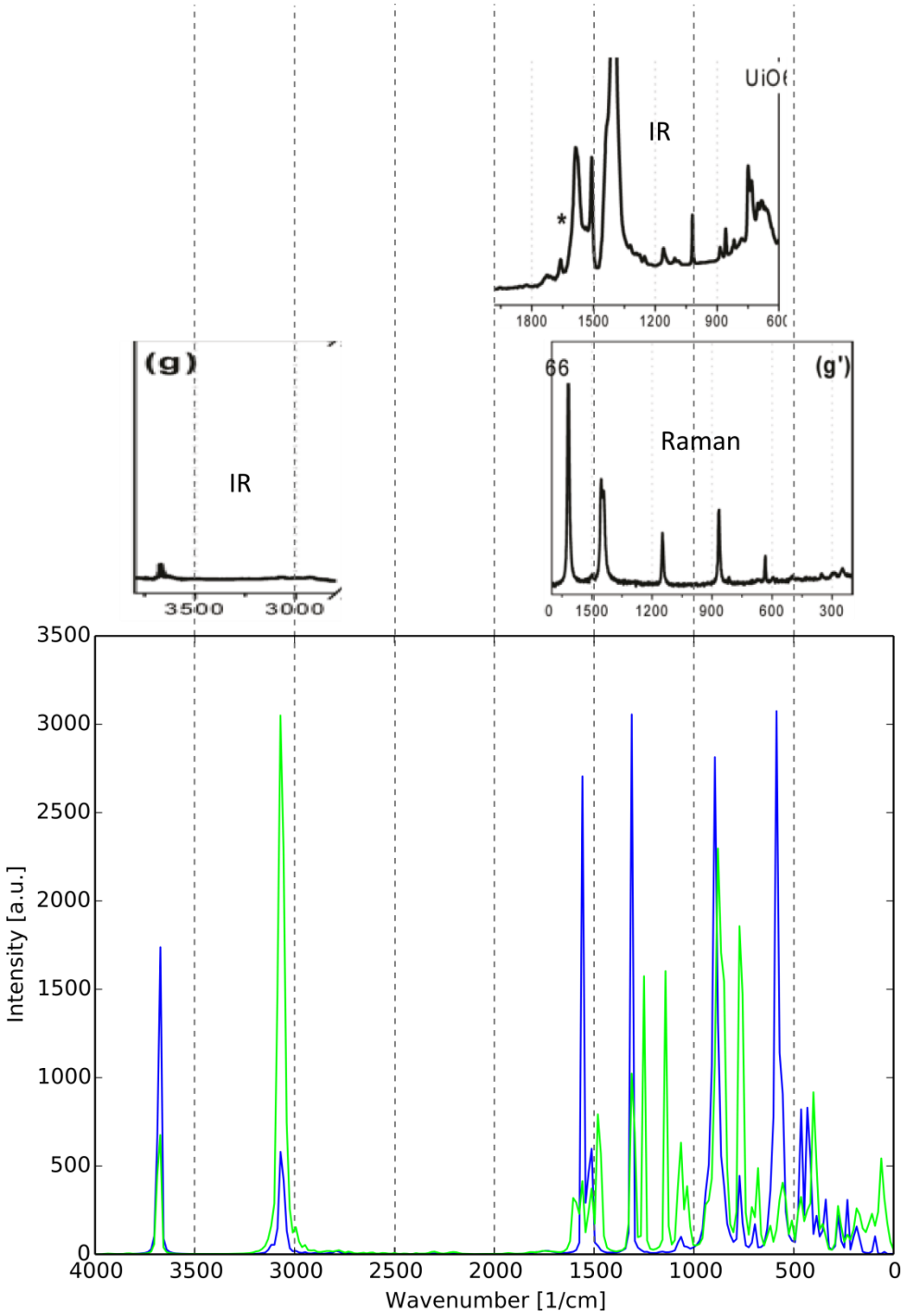

Figure 20 : Comparison of the computed IR spectrum by means of VPS (green) of a defect free UiO-66 material. The blue spectrum stands for the power spectrum of the change in dipole moment. Experimental FTIR spectra of tagged UiO-66 materials activated at 373 K have been made available by the group of Lillerud [54].

We report here the results of two recent calculations of IR spectra based on VPS as explained above. First we display an IR spectrum of NO adsorbed to copper-exchanged SSZ-13, which is known as an effective zeolitic material in the selective catalytic reduction of NO_x using ammonia. [99] Göltl et al. [99] used the theoretical model to unravel the complex multipeak infrared spectrum of NO. They performed different ab initio MD (AIMD) simulations using VASP at a finite temperature and for four

sites differing in the position of the Al-atoms and the extra-framework cation Cu^{2+}. Each site leads to a specific multi-peak IR-spectrum. In the experimental spectrum [98] shown in **Figure 18** belonging to Cu-SSZ-13 with a Si/Al ratio of 6 and Cu/Al of 0.03, three broad bands are clearly observed. Various measurements have been done at different doses of NO, which is introduced stepwise into the cell per time interval. Dependent on the dose different peaks arise or disappear. By a suitable linear combination of the theoretically obtained VPS spectra an excellent agreement with experiment is observed, as shown in **Figure 18b**. For further information we refer to ref. [99].

For a complex system with reactant molecules adsorbed at the active site of a zeolitic frame or MOF framework AIMD simulations within a periodic unit cell are only feasible for a relatively short simulation time (~ 50 ps). With the development of contemporary force fields simulations times of some nanoseconds are not exceptional and these long runs have a beneficial influence on the accuracy of reproduction of low-frequency collective modes. [101, 102] To illustrate the accuracy of current force fields we present two applications on MOFs.

In **Figure 19** the IR –spectrum of Cu-btc using the concept of the power spectrum method but with the dipole moment time derivative autocorrelation function instead of the velocity.[100] Overall, even the smaller features of the spectrum above 400 cm^{-1} are well reproduced.

As second example to illustrate the good performance of IR spectra in MOFs nowadays feasible with the current techniques is a VPS spectrum obtained after a NpT MD simulation on a defectless UiO-66 material using a force field constructed for this type of MOF following the concept of QuickFF. [103] Experimental information is given by the group of Lillerud. [54] Most of the peaks in the experimental IR spectra are well reproduced (see **Figure 20**). The peak around 3675 cm^{-1} belongs to the OH stretch while the CH stretching frequency around 3070 cm^{-1} is not clearly observed in the experimental spectrum : it is very broad with a weak intensity. The vibrational frequencies are scaled by a factor of 0.9614 which is a standard procedure to get a better comparison with observed values. The scaling accounts for both systematic errors with force constants and neglected anharmonicities.

A second leading characterization tool in zeolite chemistry (less employed in MOFs) is magic angle spinning (MAS) NMR. Silica zeolites and aluminophosphates (AlPOs) contain NMR-active elements and this makes solid-state NMR as a powerful tool for structure determination . However, in the jungle of peaks in the spectra molecular modeling is an indispensable tool to assist in unraveling the various signals. In contrast to the theoretical reproduction of IR spectra, here first-principle calculations are requisite and by preference with the help of periodic codes. We refer to a recent review on Advances in theory within the field of zeolite chemistry [35] to get an overview of the different periodic codes in which a NMR module has been implemented. Due to the overall complexity of the theoretical procedure only static approaches are suited for computation of NMR chemical shifts, limiting their direct usefulness and future in modus operandi measurements.

On the other hand optical spectroscopy has emerged as an ideal technique to study catalyst materials at work, i.e. under operando conditions. [93] UV/Vis and/or fluorescence spectroscopy can provide information about the single-molecule detection in zeolite-catalyzed reactions. [104] At the same time the breakthrough of the time-dependent form of DFT, i.e. TD-DFT, has also enabled the study of electronic excited states of relatively large systems (up to 400 atoms) , [105] making

computation of excitation and emission spectra possible with an accuracy of 0.5-0.4 eV. It has opened a lot of perspectives from the theoretical side to give insight in the interpretation of experimental spectra as measured in UV/Vis and luminescence spectroscopy. The technique has evolved in such extent that excited-state properties of large carbonaceous species can be computed which can be active intermediates in zeolite-catalyzed reactions. They can assist UV/Vis experiments combined with confocal fluorescence measurements in identifying hydrocarbon species and their location during the reaction. To illustrate the power of this relatively new characterization technique we present in **Figure 21** an assignment scale constructed from MD-averaged TD-DFT computations to assign bands in in-situ UV/Vis adsorption spectra to structurally different aromatic HP species. Despite the success of the gas phase calculations further progress is more than welcome in the theoretical description of the electronically excited state surfaces of real-life systems. To account for the full zeolitic environment further model development is needed to construct the electronic excited state surface using periodic codes, which are routinely used for the description of ground-state properties.

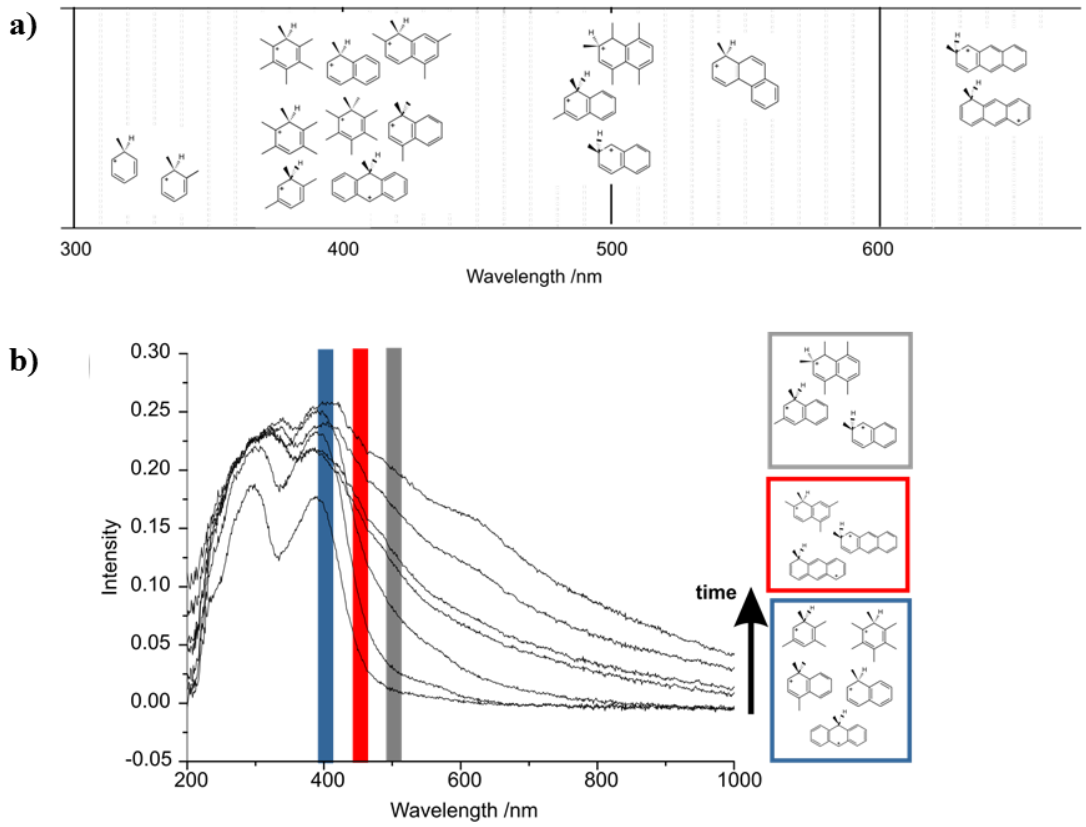

Figure 21: Assignment scale constructed from MD-averaged TD-DFT computations (a). Use of the assignment scale to assign bands in in-situ UV/Vis absorption spectra to structurally different aromatic HP species. (b). Adapted with permission from ref. [106]

6. Conclusions and perspectives

With the steady increase of new techniques to model molecular systems and chemical transformations, the expectations are growing equally. The more complexity in the system under

study, the more complexity needs to be taken into account in the model. But a model always represents some idealized description of the reality. The more complexity we insert in the model, the better we approach reality. But a phenomenon that exists in nature is governed by so many degrees of freedom, that they can never be taken into account in a model and that a serious and rational selection of external factors has to be done to keep the model as feasible.

Many obstacles have been overcome by molecular modeling, still many challenges are remaining . One of the challenges is the description of phenomena occurring at longer length and time scales and integrating information from various scales towards a unified understanding of the catalyst.

In this paper we concentrated on the techniques available to model heterogeneous catalysis under reaction conditions, which is of the highest complexity.

Enhanced MD methods have made their entrance within zeolite catalysis and also within chemical transformations in MOFs, but further progress in the methodology is still welcome as existing methods are too biased preventing the exploration of a large part of the free energy surface and neglecting the existence of some realistic pathways.

Appendix A

Chemical kinetics :

We report here some established thermodynamic expressions for the convenience of the reader. The molecular partition function Q includes in principle all electronic, translational, rotational and vibrational motions.

(i) <u>Total internal energy</u> :

$$U = RT^2 \left(\frac{\partial \ln Q}{\partial T} \right)_{N,V}$$

decomposed into: $U = U_0 + U_{therm}$

with $U_0 = E_0 = \varepsilon_0 + E_{ZPE}$ (ε_0 represents the electronic ground-state energy and $E_{ZPE} = \sum_{k=1}^{3N-6} \frac{1}{2} h\nu_k$

the zero-point energy),
and with the internal thermal energy : $U_{therm} = U_{trans} + U_{rot,ext} + U_{vib}$.

These thermal contributions can easily be evaluated with the help of Eq.(x) : $U_{trans} = \frac{3}{2} RT$;

$U_{rot,ext} = \frac{3}{2} RT$ (for a non-linear molecule) ; $U_{rot,ext} = RT$ (for a linear molcule) ;

$$U_{vib} = R \sum_{k=1}^{3N-6} \frac{h\nu_k}{k_B} \frac{1}{e^{\frac{h\nu_k}{k_B T}} - 1}$$

(ii) **<u>Enthalpy</u>** : $H = U + pV$

(iii) <u>Entropy:</u>

$$S = R\ln Q + RT\left(\frac{\partial \ln Q}{\partial T}\right)_{N,V}$$

(iv) <u>(Gibbs) free energy</u> :

$$G = H - TS$$
$$= U_0 + pV - RT\ln Q$$

Appendix B

Free energy and partition function in statistical physics :

The free energy of a system of N particles in thermodynamic equilibrium is related to its partition function (in the classical limit):

$$G = -k_B T \ln Z \tag{B1}$$

$$Z = \frac{1}{h^{3N} N!}\int d\boldsymbol{x}^N d\boldsymbol{p}^N e^{-\beta H\left(\boldsymbol{x}^N, \boldsymbol{p}^N\right)} \tag{B2}$$

Suppose we are interested in the probability distribution as function of a collective variable *s*, which may be a bond length, an angle, a coordination number,… the partition function can be rewritten in the following form:

$$Z = \int_{-\infty}^{+\infty} Z_q(s)\, ds \tag{B3}$$

with

$$Z_q(s) = \frac{1}{h^{3N} N!}\int d\boldsymbol{x}^N d\boldsymbol{p}^N \delta\left(Q\left(\boldsymbol{x}^N, \boldsymbol{p}^N\right) - s\right) e^{-\beta H\left(\boldsymbol{x}^N, \boldsymbol{p}^N\right)} \tag{B4}$$

with $Z_q(s)\,ds$ the contribution to the total partition function Z due to a microstate with a value of s in the range [s,*s+ds*]. Furthermore, one can rewrite the equation above in terms of a probability distribution $P_q(s)$:

$$P_q(s) = \frac{Z_q(s)}{Z} \quad \text{with the normalization} \quad \int_{-\infty}^{+\infty} P_q(s)\, ds = 1$$

However, if we would associate the free energy of such a microstate as:

$$G_q(s) = -k_B T \ln Z_q(s) \tag{B5}$$

- as usual - we immediately notice a dimensionality problem, because $Z_q(s)$ has the dimension of $[s]^{-1}$. One possible way to resolve this issue is by considering differences in free energies at two different values of *s*:

$$G_q(s_2) - G_q(s_1) = -k_B T \ln \frac{Z_q(s_2)}{Z_q(s_1)} = -k_B T \ln \frac{P_q(s_2)}{P_q(s_1)} \quad \left(= -k_B T \ln \frac{Z_q(s_2) ds}{Z_q(s_1) ds} \right) \tag{B6}$$

The ratio of the probability distributions in the argument of the logarithm defines whether it is more probable to find the system in the range [s_2,s_2+*ds*] than to find it in the range [s_1,s_1+*ds*], or vice versa. The ratio $\frac{P_q(s_2)}{P_q(s_1)}$ also defines whether $G_q(s_2) > G_q(s_1)$ or $G_q(s_2) < G_q(s_1)$. This is also exactly how this free energy difference should be interpreted.

Alternatively, one could define a **macrostate A** for which s lies in the range [s_1, s_2]. This gives rise to the following expressions:

$$Z_A = \int_{s_1}^{s_2} Z_q(s) ds$$

$$P_A = \frac{Z_A}{Z}$$

$$G_A = -k_B T \ln Z_A = -k_B T \ln \frac{Z_A}{Z} - k_B T \ln Z$$

$$G_A = -k_B T \ln P_A + G$$

In this case Z_A, must be interpreted as the contribution to the partition function from the macrostate A. Similarly G_A can be interpreted as the free energy associated with the macrostate A which can be computed up to a constant G, which is the total free energy. Finally, if we can assume that the partition function has a constant value of $Z_q(\bar{s})$ in that range [s_1, s_2], the equations reduce to:

$$Z_A = Z_q(\bar{s}) \Delta s$$

$$P_A = \frac{Z_q(\bar{s}) \Delta s}{Z}$$

$$G_A = -k_B T \ln Z_q(\bar{s}) \Delta s$$

with $\bar{s} = \frac{s_1 + s_2}{2}$ and $\Delta s = s_2 - s_1$

Given this background, we can now define the free energy barrier $\Delta G^{\ddagger}$ based on the one-dimensional free energy profile $G_q(s)$. We define two states: **R** representative for the reactants, and **TS** representative for the transition state region. The choice of these states can be done according to the two approaches outlined above. In the first approach, we identify **R** with the microstate corresponding to the minimum of $G_q(s)$ in the reactant valley and **TS** with the microstate corresponding to the maximum of $G_q(s)$. This gives rise to:

$$\Delta G^{\ddagger} = G_q(s_{TS}) - G_q(s_R) \quad \text{(B7)}$$

This method entails just taking the free energy difference between the maximum of the free energy profile and the minimum, which yields a very rough estimate of the free energy barrier.

References

1. Joos, L., et al., *Carbon capture turned upside down: high-temperature adsorption & low-temperature desorption (HALD).* Energy & Environmental Science, 2015. **8**(8): p. 2480-2491.
2. Kim, J., et al., *High-Throughput Characterization of Porous Materials Using Graphics Processing Units.* Journal of Chemical Theory and Computation, 2012. **8**(5): p. 1684-1693.
3. Simon, C.M., et al., *The materials genome in action: identifying the performance limits for methane storage.* Energy & Environmental Science, 2015. **8**(4): p. 1190-1199.
4. Colon, Y.J. and R.Q. Snurr, *High-throughput computational screening of metal-organic frameworks.* Chemical Society Reviews, 2014. **43**(16): p. 5735-5749.
5. Weckhuysen, B.M., *Chemical Imaging of Spatial Heterogeneities in Catalytic Solids at Different Length and Time Scales.* Angewandte Chemie-International Edition, 2009. **48**(27): p. 4910-4943.
6. Piccini, G., M. Alessio, and J. Sauer, *Ab initio Calculation of Rate Constants for Molecule–Surface Reactions with Chemical Accuracy.* Angewandte Chemie International Edition, 2016: p. n/a-n/a.
7. Svelle, S., et al., *Quantum Chemical Modeling of Zeolite-Catalyzed Methylation Reactions: Toward Chemical Accuracy for Barriers.* Journal of the American Chemical Society, 2009. **131**(2): p. 816-825.
8. Van Speybroeck, V., et al., *First Principle Kinetic Studies of Zeolite-Catalyzed Methylation Reactions.* Journal of the American Chemical Society, 2011. **133**(4): p. 888-899.
9. Sauer, J. and H.-J. Freund, *Models in Catalysis.* Catalysis Letters, 2015. **145**(1): p. 109-125.
10. De Wispelaere, K., S. Bailleul, and V. Van Speybroeck, *Towards molecular control of elementary reactions in zeolite catalysis by advanced molecular simulations mimicking operating conditions.* Catalysis Science & Technology, 2016. **6**(8): p. 2686-2705.
11. De Wispelaere, K., et al., *Complex Reaction Environments and Competing Reaction Mechanisms in Zeolite Catalysis: Insights from Advanced Molecular Dynamics.* Chemistry – A European Journal, 2015. **21**(26): p. 9385-9396.
12. De Wispelaere, K., et al., *Insight into the Effect of Water on the Methanol-to-Olefins Conversion in H-SAPO-34 from Molecular Simulations and in Situ Microspectroscopy.* ACS Catalysis, 2016. **6**: p. 1991-2002.
13. Moors, S.L.C., et al., *Molecular Dynamics Kinetic Study on the Zeolite-Catalyzed Benzene Methylation in ZSM-5.* Acs Catalysis, 2013. **3**(11): p. 2556-2567.
14. Van der Mynsbrugge, J., et al., *Insight into the Formation and Reactivity of Framework-Bound Methoxide Species in H-ZSM-5 from Static and Dynamic Molecular Simulations.* Chemcatchem, 2014. **6**(7): p. 1906-1918.
15. Benco, L., T. Bucko, and J. Hafner, *Dehydrogenation of propane over Zn-MOR. Static and dynamic reaction energy diagram.* Journal of Catalysis, 2011. **277**(1): p. 104-116.
16. Bucko, T., et al., *Mechanism of alkane dehydrogenation catalyzed by acidic zeolites: Ab initio transition path sampling.* Journal of Chemical Physics, 2009. **131**(21): p. 11.
17. Bucko, T., et al., *Monomolecular cracking of propane over acidic chabazite: An ab initio molecular dynamics and transition path sampling study.* Journal of Catalysis, 2011. **279**(1): p. 220-228.

18. Bučko, T. and J. Hafner, *The role of spatial constraints and entropy in the adsorption and transformation of hydrocarbons catalyzed by zeolites.* Journal of Catalysis, 2015. **329**(0): p. 32-48.
19. Goltl, F. and J. Hafner, *Modelling the adsorption of short alkanes in protonated chabazite: The impact of dispersion forces and temperature.* Microporous and Mesoporous Materials, 2013. **166**(0): p. 176-184.
20. Jiang, T., et al., *Effect of Temperature on the Adsorption of Short Alkanes in the Zeolite SSZ-13—Adapting Adsorption Isotherms to Microporous Materials.* ACS Catalysis, 2014. **4**(7): p. 2351-2358.
21. Gomes, J., M. Head-Gordon, and A.T. Bell, *Reaction Dynamics of Zeolite-Catalyzed Alkene Methylation by Methanol.* Journal of Physical Chemistry C, 2014. **118**(37): p. 21409-21419.
22. Zimmerman, P.M., et al., *Ab Initio Simulations Reveal that Reaction Dynamics Strongly Affect Product Selectivity for the Cracking of Alkanes over H-MFI.* Journal of the American Chemical Society, 2012. **134**(47): p. 19468-19476.
23. Van Speybroeck, V., et al., *First principle chemical kinetics in zeolites: the methanol-to-olefin process as a case study.* Chemical Society Reviews, 2014. **43**(21): p. 7326-7357.
24. Corma, A., *State of the art and future challenges of zeolites as catalysts.* Journal of Catalysis, 2003. **216**(1-2): p. 298-312.
25. Rowsell, J.L.C. and O.M. Yaghi, *Metal-organic frameworks: a new class of porous materials.* Microporous and Mesoporous Materials, 2004. **73**(1-2): p. 3-14.
26. Ferey, G., *Hybrid porous solids: past, present, future.* Chemical Society Reviews, 2008. **37**(1): p. 191-214.
27. Vermoortele, F., et al., *Electronic Effects of Linker Substitution on Lewis Acid Catalysis with Metal-Organic Frameworks.* Angewandte Chemie-International Edition, 2012. **51**(20): p. 4887-4890.
28. Maihom, T., et al., *Reaction Mechanisms of the Methylation of Ethene with Methanol and Dimethyl Ether over H-ZSM-5: An ONIOM Study.* Journal of Physical Chemistry C, 2009. **113**(16): p. 6654-6662.
29. Dapprich, S., et al., *A new ONIOM implementation in Gaussian98. Part I. The calculation of energies, gradients, vibrational frequencies and electric field derivatives.* Journal of Molecular Structure-Theochem, 1999. **461**: p. 1-21.
30. Bulo, R.E., et al., *Toward a Practical Method for Adaptive QM/MM Simulations.* Journal of Chemical Theory and Computation, 2009. **5**(9): p. 2212-2221.
31. Gomes, J., et al., *Accurate Prediction of Hydrocarbon interactions with Zeolites Utilizing improved Exchange-Correlation Functionals and QM/MM Methods: Benchmark Calculations of Adsorption Enthalpies and Application to Ethene Methylation by Methanol.* Journal of Physical Chemistry C, 2012. **116**(29): p. 15406-15414.
32. Tranca, D.C., et al., *Hexane Cracking on ZSM-5 and Faujasite Zeolites: a QM/MM/QCT Study.* The Journal of Physical Chemistry C, 2015. **119**(52): p. 28836-28853.
33. Nieminen, V., et al., *Stabilities of C3–C5 alkoxide species inside H-FER zeolite: a hybrid QM/MM study.* Journal of Catalysis, 2005. **231**(2): p. 393-404.
34. Grimme, S., et al., *A consistent and accurate ab initio parametrization of density functional dispersion correction (DFT-D) for the 94 elements H-Pu.* Journal of Chemical Physics, 2010. **132**(15): p. 154104.
35. Van Speybroeck, V., et al., *Advances in theory and their application within the field of zeolite chemistry.* Chemical Society Reviews, 2015. **44**(20): p. 7044-7111.
36. Notari, B., *Microporous crystalline titanium silicates*, in *Advances in Catalysis, Vol 41*, D.D. Eley, W.O. Haag, and B. Gates, Editors. 1996. p. 253-334.
37. Prokopyeva, I., et al., *Suppression of Aromatic Cycle in Methanol-to- Olefins Reaction over ZSM-5 by post-synthetic modification using Calcium.* ChemCatChem, 2016.

38. Dedecek, J., D. Kaucky, and B. Wichterlova, *Al distribution in ZSM-5 zeolites: an experimental study.* Chemical Communications, 2001(11): p. 970-971.
39. Sklenak, S., et al., *Aluminum siting in silicon-rich zeolite frameworks: A combined high-resolution Al-27 NMR spectroscopy and quantum mechanics/molecular mechanics study of ZSM-5.* Angewandte Chemie-International Edition, 2007. **46**(38): p. 7286-7289.
40. Sklenak, S., et al., *Aluminium siting in the ZSM-5 framework by combination of high resolution Al-27 NMR and DFT/MM calculations.* Physical Chemistry Chemical Physics, 2009. **11**(8): p. 1237-1247.
41. Van der Mynsbrugge, J., et al., *Methylation of benzene by methanol: Single-site kinetics over H-ZSM-5 and H-beta zeolite catalysts.* Journal of Catalysis, 2012. **292**: p. 201-212.
42. Van der Mynsbrugge, J., et al., *Efficient Approach for the Computational Study of Alcohol and Nitrile Adsorption in H-ZSM-5.* Journal of Physical Chemistry C, 2012. **116**(9): p. 5499-5508.
43. Lo, C., et al., *Methanol coupling in the zeolite chabazite studied via Car-Parrinello molecular dynamics.* Molecular Physics, 2004. **102**(3): p. 281-288.
44. Sauer, J., M. Sierka, and F. Haase, *Acidic Catalysis by Zeolites. Ab Initio Modeling of Transition Structures*, in *Transitions State Modeling for Catalysis*, K. Morokuma and D.G. Truhlar, Editors. 1999, American Chemical Society: Washington DC. p. 358-367.
45. Haase, F., J. Sauer, and J. Hutter, *Ab initio molecular dynamics simulation of methanol adsorbed in chabazite.* Chemical Physics Letters, 1997. **266**(3-4): p. 397-402.
46. Stich, I., et al., *Role of the zeolitic environment in catalytic activation of methanol.* Journal of the American Chemical Society, 1999. **121**(14): p. 3292-3302.
47. Gale, J.D., et al., *Methanol in microporous materials from first principles.* Catalysis Today, 1999. **50**(3-4): p. 525-532.
48. Termath, V., et al., *Understanding the nature of water bound to solid acid surfaces. Ab initio simulation on HSAPO-34.* Journal of the American Chemical Society, 1998. **120**(33): p. 8512-8516.
49. Jeanvoine, Y., et al., *Bronsted acid sites in HSAPO-34 and chabazite: An ab initio structural study.* Journal of Physical Chemistry B, 1998. **102**(29): p. 5573-5580.
50. Vener, M.V., X. Rozanska, and J. Sauer, *Protonation of water clusters in the cavities of acidic zeolites: (H2O)(n)center dot H-chabazite, n=1-4.* Physical Chemistry Chemical Physics, 2009. **11**(11): p. 1702-1712.
51. Joshi, K.L., et al., *Reactive molecular simulations of protonation of water clusters and depletion of acidity in H-ZSM-5 zeolite.* Physical Chemistry Chemical Physics, 2014. **16**(34): p. 18433-18441.
52. Cavka, J.H., et al., *A new zirconium inorganic building brick forming metal organic frameworks with exceptional stability.* Journal of the American Chemical Society, 2008. **130**(42): p. 13850-13851.
53. Guillerm, V., et al., *A zirconium methacrylate oxocluster as precursor for the low-temperature synthesis of porous zirconium(IV) dicarboxylates.* Chemical Communications, 2010. **46**(5): p. 767-769.
54. Kandiah, M., et al., *Synthesis and Stability of Tagged UiO-66 Zr-MOFs.* Chemistry of Materials, 2010. **22**(24): p. 6632-6640.
55. Vandichel, M., et al., *Active site engineering of UiO-66 type metal-organic frameworks by intentional creation of defects: A theoretical rationalization.* CrystEngComm, 2015. **17**: p. 395-406.
56. Hajek, J., et al., *Mechanistic studies of aldol condensations in UiO-66 and UiO-66-NH2 metal organic frameworks.* Journal of Catalysis, 2015. **331**: p. 1-12.
57. Cliffe, M.J., et al., *Correlated defect nanoregions in a metal-organic framework.* Nat Commun, 2014. **5**: p. 4176.
58. Oien, S., et al., *Detailed Structure Analysis of Atomic Positions and Defects in Zirconium Metal-Organic Frameworks.* Crystal Growth & Design, 2014. **14**(11): p. 5370-5372.

59. Trickett, C.A., et al., *Definitive Molecular Level Characterization of Defects in UiO-66 Crystals.* Angewandte Chemie-International Edition, 2015. **54**(38): p. 11162-11167.
60. Ling, S. and B. Slater, *Dynamic Acidity in Defective UiO-66.* Chemical Science, 2016: p. in press.
61. Vandichel, M., et al., *Water coordination and dehydroxylation processes in defective UiO-66 type metal-organic frameworks.* CrystEngComm, 2016. **submitted**.
62. Kresse, G. and J. Furthmuller, *Efficient iterative schemes for ab initio total-energy calculations using a plane-wave basis set.* Physical Review B, 1996. **54**(16): p. 11169-11186.
63. Kresse, G. and J. Furthmüller, *Efficiency of ab-initio total energy calculations for metals and semiconductors using a plane-wave basis set.* Comput. Mat. Sci., 1996. **6**: p. 15.
64. Kresse, G. and J. Hafner, *ABINITIO MOLECULAR-DYNAMICS FOR LIQUID-METALS.* Physical Review B, 1993. **47**(1): p. 558-561.
65. Kresse, G. and J. Hafner, *Ab initio molecular-dynamics simulation of the liquid-metal-amorphous-semiconductor transition in germanium.* Phys. Rev. B, 1994. **49**: p. 14251.
66. Bhan, A., et al., *DFT investigation of alkoxide formation from olefins in H-ZSM-5.* Journal of Physical Chemistry B, 2003. **107**(38): p. 10476-10487.
67. Ishikawa, H., et al., *Stable dimerized alkoxy species of 2-methylpropene on mordenite zeolite studied by FT-IR.* Journal of Physical Chemistry B, 1999. **103**(27): p. 5681-5686.
68. Kondo, J.N., et al., *IR study of adsorption and reaction of 1-butene on H-ZSM-5.* Catalysis Letters, 1997. **47**(2): p. 129-133.
69. Nguyen, C.M., et al., *Physisorption and Chemisorption of Linear Alkenes in Zeolites: A Combined QM-Pot(MP2//B3LYP:GULP)-Statistical Thermodynamics Study.* Journal of Physical Chemistry C, 2011. **115**(48): p. 23831-23847.
70. Boronat, M., P.M. Viruela, and A. Corma, *Reaction Intermediates in Acid Catalysis by Zeolites: Prediction of the Relative Tendency To Form Alkoxides or Carbocations as a Function of Hydrocarbon Nature and Active Site Structure.* Journal of the American Chemical Society, 2004. **126**(10): p. 3300-3309.
71. Kondo, J.N., F. Wakabayashi, and K. Domen, *IR Study of Adsorption of Olefins on Deuterated ZSM-5.* The Journal of Physical Chemistry B, 1998. **102**(12): p. 2259-2262.
72. Frenkel, D. and B. Smit, *Understanding Molecular Simulations*. second edition ed. 2002: Academic press, Elsevier.
73. Hajek, J., et al., *On the stability and nature of adsorbed pentene in Brønsted acid zeolite H-ZSM-5 at 323 K.* Journal of Catalysis, 2016. **340**: p. 227-235.
74. Goeltl, F., et al., *Van der Waals interactions between hydrocarbon molecules and zeolites: Periodic calculations at different levels of theory, from density functional theory to the random phase approximation and Moller-Plesset perturbation theory.* Journal of Chemical Physics, 2012. **137**(11): p. 114111.
75. De Wispelaere, K., et al., *Complex Reaction Environments and Competing Reaction Mechanisms in Zeolite Catalysis: Insights from Advanced Molecular Dynamics.* Chemistry-a European Journal, 2015. **21**(26): p. 9385-9396.
76. Perdew, J.P., K. Burke, and M. Ernzerhof, *Generalized gradient approximation made simple (vol 77, pg 3865, 1996).* Physical Review Letters, 1997. **78**(7): p. 1396-1396.
77. Yang, K., et al., *Tests of the RPBE, revPBE, tau-HCTHhyb, omega B97X-D, and MOHLYP density functional approximations and 29 others against representative databases for diverse bond energies and barrier heights in catalysis.* Journal of Chemical Physics, 2010. **132**(16): p. 10.
78. Wellendorff, J., et al., *Density functionals for surface science: Exchange-correlation model development with Bayesian error estimation.* Physical Review B, 2012. **85**(23): p. 235149.
79. Ambrosetti, A., et al., *Long-range correlation energy calculated from coupled atomic response functions.* Journal of Chemical Physics, 2014. **140**(18).

80. Bučko, T., et al., *Many-body dispersion corrections for periodic systems: an efficient reciprocal space implementation.* Journal of Physics: Condensed Matter, 2016. **28**(4): p. 045201.
81. Aryasetiawan, F., T. Miyake, and K. Terakura, *Total energy method from many-body formulation.* Physical Review Letters, 2002. **88**(16): p. 166401.
82. Goltl, F. and J. Hafner, *Alkane adsorption in Na-exchanged chabazite: The influence of dispersion forces.* Journal of Chemical Physics, 2011. **134**(6): p. 064102.
83. Frisch, M.J., et al., *Gaussian 09, {R}evision {A}.02*. 2009, Gaussian, Inc., Wallingford CT.
84. Jones, A.J. and E. Iglesia, *Kinetic, Spectroscopic, and Theoretical Assessment of Associative and Dissociative Methanol Dehydration Routes in Zeolites.* Angewandte Chemie International Edition, 2014. **53**(45): p. 12177-12181.
85. Brogaard, R.Y., et al., *Methanol-to-hydrocarbons conversion: The alkene methylation pathway.* Journal of Catalysis, 2014. **314**(0): p. 159-169.
86. Laio, A. and F.L. Gervasio, *Metadynamics: a method to simulate rare events and reconstruct the free energy in biophysics, chemistry and material science.* Reports on Progress in Physics, 2008. **71**(12): p. 22.
87. Laio, A. and M. Parrinello, *Escaping free-energy minima.* Proceedings of the National Academy of Sciences of the United States of America, 2002. **99**(20): p. 12562-12566.
88. Bolhuis, P.G., et al., *Transition path sampling: Throwing ropes over rough mountain passes, in the dark.* Annual Review of Physical Chemistry, 2002. **53**: p. 291-318.
89. Dellago, C., P.G. Bolhuis, and P.L. Geissler, *Transition path sampling.* Advances in Chemical Physics, Vol 123, 2002. **123**: p. 1-78.
90. Bucko, T., et al., *Mechanism of alkane dehydrogenation catalyzed by acidic zeolites: Ab initio transition path sampling.* Journal of Chemical Physics, 2009. **131**(21): p. 214508.
91. Ensing, B., *Chemistry in Water, First Principles Computer Simulations.* PhD thesis, 2013.
92. Ensing, B., et al., *A recipe for the computation of the free energy barrier and the lowest free energy path of concerted reactions.* Journal of Physical Chemistry B, 2005. **109**(14): p. 6676-6687.
93. Weckhuysen, B.M., *Preface: recent advances in the in-situ characterization of heterogeneous catalysts.* Chemical Society Reviews, 2010. **39**(12): p. 4557-4559.
94. Silaghi, M.-C., et al., *Dealumination mechanisms of zeolites and extra-framework aluminum confinement.* Journal of Catalysis, 2016. **339**: p. 242-255.
95. Brogaard, R.Y., B.M. Weckhuysen, and J.K. Norskov, *Guest-host interactions of arenes in H-ZSM-5 and their impact on methanol-to-hydrocarbons deactivation processes.* Journal of Catalysis, 2013. **300**: p. 235-241.
96. Piccini, G. and J. Sauer, *Effect of Anharmonicity on Adsorption Thermodynamics.* Journal of Chemical Theory and Computation, 2014. **10**(6): p. 2479-2487.
97. Bornhauser, P. and D. Bougeard, *Intensities of the vibrational spectra of siliceous zeolites by molecular dynamics calculations. I. Infrared spectra.* Journal of Physical Chemistry B, 2001. **105**(1): p. 36-41.
98. Zhang, R., et al., *NO Chemisorption on Cu/SSZ-13: A Comparative Study from Infrared Spectroscopy and DFT Calculations.* Acs Catalysis, 2014. **4**(11): p. 4093-4105.
99. Goeltl, F., P. Sautet, and I. Hermans, *Can Dynamics Be Responsible for the Complex Multipeak Infrared Spectra of NO Adsorbed to Copper(II) Sites in Zeolites?* Angewandte Chemie-International Edition, 2015. **54**(27): p. 7799-7804.
100. Tafipolsky, M., S. Amirjalayer, and R. Schmid, *First-Principles-Derived Force Field for Copper Paddle-Wheel-Based Metal-Organic Frameworks.* Journal of Physical Chemistry C, 2010. **114**(34): p. 14402-14409.
101. Bueno-Perez, R., et al., *Zeolite Force Fields and Experimental Siliceous Frameworks in a Comparative Infrared Study.* Journal of Physical Chemistry C, 2012. **116**(49): p. 25797-25805.

102. Maurin, G., et al., *Theoretical prediction of low-frequency vibrations of extra-framework cations in mordenite zeolites.* Physical Chemistry Chemical Physics, 2004. **6**(1): p. 182-187.
103. Vanduyfhuys, L., et al., *QuickFF: A Program for a Quick and Easy Derivation of Force Fields for Metal-Organic Frameworks from Ab Initio Input.* Journal of Computational Chemistry, 2015. **36**(13): p. 1015-1027.
104. Janssen, K.P.F., et al., *Single molecule methods for the study of catalysis: from enzymes to heterogeneous catalysts.* Chemical Society Reviews, 2014. **43**(4): p. 990-1006.
105. Adamo, C. and D. Jacquemin, *The calculations of excited-state properties with Time-Dependent Density Functional Theory.* Chemical Society Reviews, 2013. **42**(3): p. 845-856.
106. Hemelsoet, K., et al., *Identification of Intermediates in Zeolite-Catalyzed Reactions by In Situ UV/Vis Microspectroscopy and a Complementary Set of Molecular Simulations.* Chemistry-a European Journal, 2013. **19**(49): p. 16595-16606.